detected in any of the three mutants due to the low sensitivity of this technique (data not shown).

Infectivity of ZF mutant viruses and proviral DNA synthesis

We next determined whether or not the mutant DNA plasmids produced infectious virus. CD4-positive M8166 cells were infected with the supernatants of transfected Cos-1 cells containing equal amounts of viral RNAs, as measured by quantitative RT-PCR. Conspicuous syncytium formation was observed in the M8166 cells infected with the supernatant from cells transfected with WT DNA. The culture supernatant of these cells accumulated RT activity. In contrast, there was no indication of infectivity in the cells infected with the supernatants from the three mutant DNAs during the observation period of more than 1 month. Thus, alteration of the ZF motifs resulted in total loss of viral infectivity.

According to a recent report (Guo *et al.*, 1997), alterations in ZF motifs appear to affect not only the packaging ability of genomic RNA but also the ability to synthesize DNA at the step of strand transfer. To analyse DNA synthesis in SIVmac, we determined the levels of the different forms of DNA (Fig. 4A) by PCR. The genomic DNA was extracted from M8166 cells 4, 8 and 48 h after infection with the WT and mutant viruses containing the same amount of viral RNA, and five different regions were amplified to monitor to which step viral DNA synthesis proceeded: (i) R/U5 LTR (synthesis of −ssDNA); (ii) U3/U5 (synthesis of minus-strand DNA after minus-strand transfer); (iii) MA/CA (synthesis of the end of minus-strand); (iv) U3/CA (synthesis of the plus-strand DNA after plus-strand transfer); or (v) 2-LTR form. As shown in Fig. 4(B), −ssDNA was synthesized in the WT and all mutant viruses. After the step of minus-strand transfer, synthesis of the minus-strand DNA was completed in all the viruses. Interestingly, after the plus-strand transfer, synthesis of the plus-strand DNA failed in all the mutants. The 2-LTR form was not detected in any of the mutants, while it was detected in the WT at 48 h post-infection (data not shown). The detection limit of the PCRs (i)–(v) was found to be 100 copies of the target molecules in a reaction mixture by measuring serially diluted standard solutions of the parental plasmid (a representative result is given in Fig. 4C). The results indicated that the ZF motifs contribute to the efficient synthesis of viral DNA at the step of plus-strand transfer and that the roles of ZF1 and ZF2 were almost the same. Thus, all the SIVmac ZF mutants appeared to be non-infectious due to inefficient or incomplete synthesis of viral DNA.

DISCUSSION

In our previous analysis of HIV-1 NC (Mizuno *et al.*, 1996), the first two cysteine residues in both ZF1 and ZF2 mutants (HIV-1 ZF1* and HIV-1 ZF2*) were replaced by serine residues. In this study, we modified the ZF motifs of SIVmac in the same way to compare the functions of the two motifs in HIV-1 and SIVmac. The genomic RNA content of HIV-1 ZF1* was about 10 % that of the WT, whereas the genomic RNA content of HIV-1 ZF2* was almost as much as that of the WT. An immunoblot analysis of the virus particles showed that HIV-1 ZF2* particles contained some proteins with smaller molecular sizes than expected. These were thought to be degradation products of $p27^{CA}$. HIV-1 ZF1* particles did not appear to have such degradation products. These results indicated that the ZF1 of HIV-1 is primarily responsible for RNA encapsidation while ZF2 is required for stabilization of virus particles.

The present results contrast with these previous results obtained for HIV-1. SIVmac ZF1* and ZF2* had approximately the same reduction in genomic RNA content compared with the WT. The genomic RNA content of SIVmac ZF1* was about 26 % and SIVmac ZF2* was about 20 % that of the WT. These results indicate that the two ZF motifs of SIVmac239 NC protein function almost equivalently with respect to RNA encapsidation. It also means that ZF2 of SIVmac might bind the genomic RNA slightly more strongly than ZF1. Urbaneja *et al.* (2000) reported that, with respect to the isolated SIVmne ZF1 and ZF2 peptides, their intensity of binding to nucleic acids was close to half that seen for SIVmne NCp8 and that the SIVmne ZF2 peptide bound the nucleic acids slightly more strongly than the SIVmne ZF1 peptide. The finding of this report is thus similar to our result. Yovandich *et al.* (2001) reported that the SIVmne ZF2 mutant resulted in an approximately 30 % reduction in the level of genomic RNA, while the SIVmne ZF1 mutant had a genomic RNA similar to that of the WT virion. They suggested that SIVmne ZF2 appears to function more significantly in genomic RNA encapsidation than SIVmne ZF1. With respect to the encapsidation of genomic RNA in HIV-2, both ZF1 and ZF2 motifs interact specifically with viral RNA (Komatsu *et al.*, 1996), which is in marked contrast to HIV-1, where the ZF2 motif does not interact specifically with viral RNA (De Rocquigny *et al.*, 1992; Mizuno *et al.*, 1996). The functions of the two ZFs of HIV-2 are thus similar to those of SIVmac. This similarity is not surprising since SIVs are genetically more closely related to HIV-2 than to HIV-1. An immunoblot analysis of the transfected cells showed that SIVmac ZF1* and ZF2* expressed the Gag precursor protein, Pr46, at approximately the same level, indicating that the ZF motifs of SIVmac239 NC protein function almost equivalently with respect to the processing of Gag precursors, as well as RNA encapsidation. These results also suggest that the functions of the two ZFs in SIVmac are slightly different from those in HIV-1. Interestingly, it has been reported that HIV-1 and HIV-2 differ in the process of genomic RNA packaging (Kaye & Lever, 1999), with genomic RNA being captured in *trans* in HIV-1, whereas unspliced RNA is selected in *cis* by the Gag protein in HIV-2. We cannot tell whether that is true or not from our results, but we consider that the difference in selection of genomic RNA might be related to the difference in the ZF functions between HIV-1 and HIV-2/SIV.

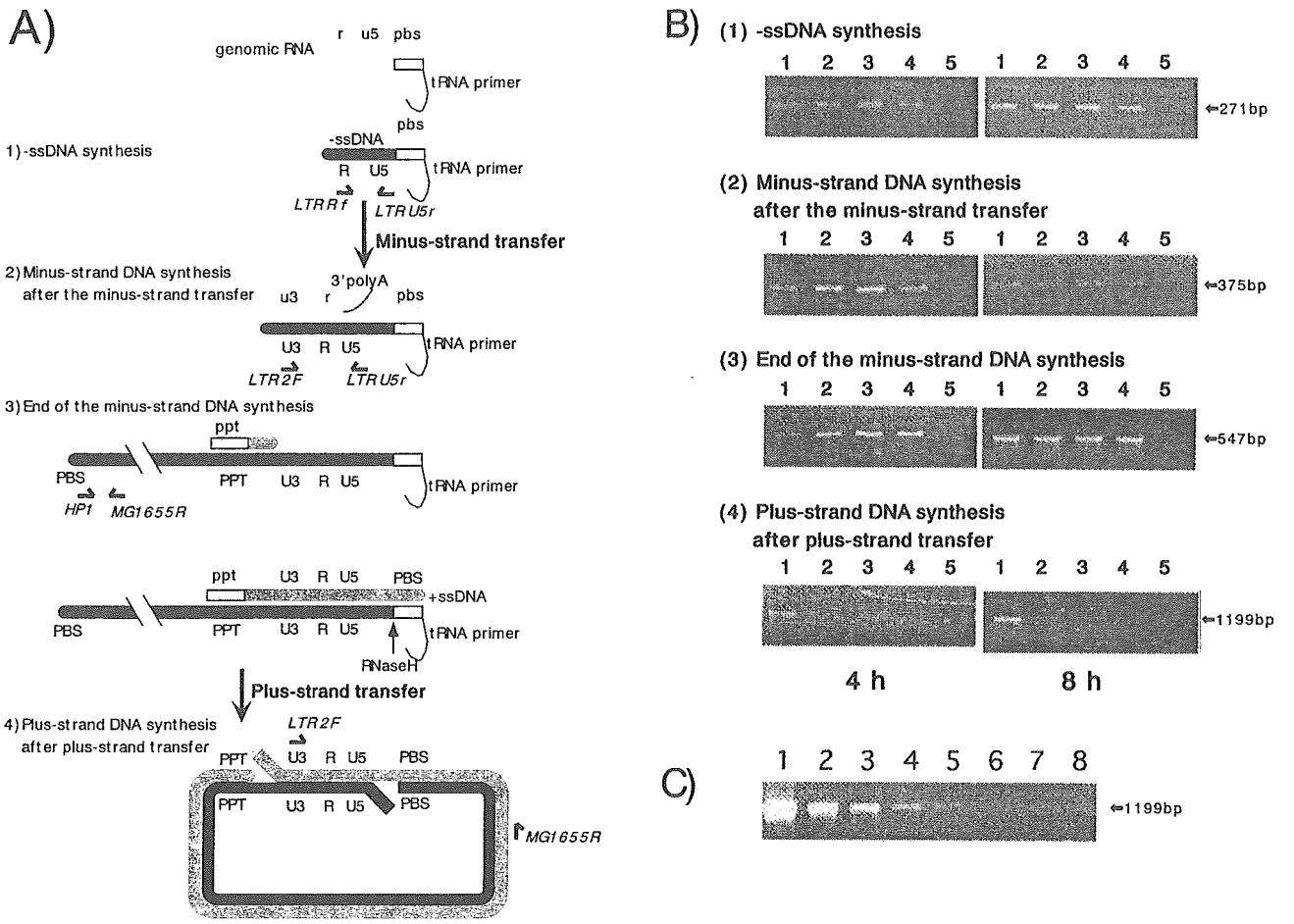

Fig. 4. PCR analysis of the four steps of viral DNA synthesis. (A) Schematic drawings of the steps: (i) −ssDNA synthesis, which is detected by the LTR Rf/LTR U5r primer pair; (ii) minus-strand DNA synthesis after the minus-strand transfer, which is detected by the LTR 2F/LTR U5r primer pair; (iii) the end of the minus-strand DNA synthesis, which is detected by the HP1/MG1655R primer pair; and (iv) plus-strand DNA synthesis after the plus-strand transfer, which is detected by the LTR 2F/MG1655R primer pair. Primer pairs are shown in italics and their complementary sequences are shown by horizontal arrows. (B) PCR results obtained for each of the four steps using M8166 cells 4 h (left panels) and 8 h (right panels) after being infected with the WT and mutant viruses. The amount of each type of virus used to infect the cells was the same. Lane 1, WT; lane 2, SIVmac ZF1*; lane 3, SIVmac ZF2*; lane 4, SIVmac ZF1*2*; lane 5, mock-infected cells. (C) Sensitivity of the PCR used in the analysis of DNA synthesis. Quantified copy numbers of SIVmac plasmid (pMA239) were amplified with U3/CA viral DNA detection primers LTR 2F and MG1655R, which detect elongation of plus-strand DNA after the plus-strand transfer. Lanes 1–8 correspond to copy numbers of 10^8, 10^6, 10^4, 10^3, 10^2, 10, 1 and 0, respectively.

In order to distinguish between a drop in packaging efficiency and a decrease in the amount of RNA available for encapsidation as a result of the mutations in the ZF motifs, we measured the genomic RNA levels in the cell lysates. We found no significant differences in the RNA levels of the three mutants and the WT, indicating that the introduction of mutations in the ZF motifs did not cause a drop in the levels of genome RNA available for encapsidation.

It can thus be concluded that mutagenesis in the ZF motifs of SIVmac NC protein resulted in loss of viral infectivity, and that this loss was partly attributable to a reduction in the packaging efficiency of genomic RNA. However, this does not explain fully the results, since the ZF mutant viruses lost all viral infectivity, even though they retained some genomic RNA (20 % or higher). In this context it is noteworthy that SIVmne ZF mutants with no viral infectivity produced immature or morphologically aberrant particles (Gorelick *et al.*, 1999; Yovandich *et al.*, 2001) which retained genomic RNA to some extent (some contained almost WT levels of genomic RNA). To elucidate the reason for this, we focused on the roles of the ZF motifs of SIVmac NC in viral DNA synthesis. In fact, the NCs of MuLV and HIV-1 are reported to increase the efficiency of synthesis of DNA products (Allain *et al.*, 1994; Berthoux *et al.*, 1997; Gonsky *et al.*, 2001; Gorelick *et al.*, 1996; Wu *et al.*, 1999; You & McHenry, 1994; Yu & Darlix, 1996). Guo *et al.* (1997) reported that alterations in ZF motifs of HIV-1 NC affected the ability to

synthesize DNA at the step of strand transfer. Recently Guo *et al.* (2000), using an *in vitro* model system, reported that the ZF motifs of HIV-1 NC were required for efficient minus- and plus-strand transfer and that these motifs were involved in the reaction by which NC completely removes the tRNA primer during plus-strand transfer. In this study, it was clarified that the minus-strand transfer was completed, but the plus-strand transfer seemed to have failed in all the ZF mutants of SIVmac. This finding suggests that the mutations in ZF motifs of SIVmac led to a loss of infectivity partly because of impairment of DNA synthesis. The removal of tRNA primer during the plus-strand transfer might be a critical step in the replication of all the SIV ZF mutants, since the presence of the tRNA primer attatched to the template RNA genome obviously blocks a smooth move to the next step of elongation of plus-strand DNA synthesis.

In conclusion, the present study has revealed that the ZF motifs of SIVmac NC protein are required in the final step of DNA synthesis, suggesting an important role for the NC protein in viral DNA synthesis, in addition to its importance in genome packaging, which is perhaps not surprising considering that it is the protein that interacts most closely with genomic RNA. Further studies of how NC proteins of HIV and SIV perform these multiple tasks, especially at the molecular level, are necessary to understand fully the mechanism of replication of the primate lentiviruses.

ACKNOWLEDGEMENTS

We are grateful to Drs Takeo Kuwata, Masahiro Yamashita and Yoshimi Enose for many technical suggestions. This work was supported by Health Science Research Grants from the Ministry of Health, Labor and Welfare and a Grant-in-Aid for Scientific Research from the Ministry of Education and Science.

REFERENCES

Akahata, W., Ido, E., Shimada, T., Katsuyama, K., Yamamoto, H., Uesaka, H., Ui, M., Kuwata, T., Takahashi, H. & Hayami, M. (2000). DNA vaccination of macaques by a full genome HIV-1 plasmid which produces noninfectious virus particles. *Virology* 275, 116–124.

Aldovini, A. & Young, R. A. (1990). Mutations of RNA and protein sequences involved in human immunodeficiency virus type 1 packaging result in production of noninfectious virus. *J Virol* 64, 1920–1926.

Allain, B., Lapadat-Tapolsky, M., Berlioz, C. & Darlix, J. L. (1994). Transactivation of the minus-strand DNA transfer by nucleocapsid protein during reverse transcription of the retroviral genome. *EMBO J* 13, 973–981.

Barat, C., Lullien, V., Schatz, O., Keith, G., Nugeyre, M. T., Gruninger-Leitch, F., Barre-Sinoussi, F., LeGrice, S. F. & Darlix, J. L. (1989). HIV-1 reverse transcriptase specifically interacts with the anticodon domain of its cognate primer tRNA. *EMBO J* 8, 3279–3285.

Barat, C., Schatz, O., LeGrice, S. & Darlix, J. L. (1993). Analysis of the interactions of HIV1 replication primer $tRNA^{Lys,3}$ with nucleocapsid protein and reverse transcriptase. *J Mol Biol* 231, 185–190.

Berg, J. M. (1986). Potential metal-binding domains in nucleic acid binding proteins. *Science* 232, 485–487.

Berkowitz, R. D., Luban, J. & Goff, S. P. (1993). Specific binding of human immunodeficiency virus type 1 gag polyprotein and nucleocapsid protein to viral RNAs detected by RNA mobility shift assays. *J Virol* 67, 7190–7200.

Berthoux, L., Pechoux, C., Ottmann, M., Morel, G. & Darlix, J. L. (1997). Mutations in the N-terminal domain of human immunodeficiency virus type 1 nucleocapsid protein affect virion core structure and proviral DNA synthesis. *J Virol* 71, 6973–6981.

Covey, S. N. (1986). Amino acid sequence homology in gag region of reverse transcribing elements and the coat protein gene of cauliflower mosaic virus. *Nucleic Acids Res* 14, 623–633.

Dannull, J., Surovoy, A., Jung, G. & Moelling, K. (1994). Specific binding of HIV-1 nucleocapsid protein to PSI RNA in vitro requires N-terminal zinc finger and flanking basic amino acid residues. *EMBO J* 13, 1525–1533.

Darlix, J. L., Lapadat-Tapolsky, M., De Rocquigny, H. & Roques, B. P. (1995). First glimpses at structure–function relationships of the nucleocapsid protein of retroviruses. *J Mol Biol* 254, 523–537.

De Rocquigny, H., Gabus, C., Vincent, A., Fournie-Zaluski, M. C., Roques, B. & Darlix, J. L. (1992). Viral RNA annealing activities of human immunodeficiency virus type 1 nucleocapsid protein require only peptide domains outside the zinc fingers. *Proc Natl Acad Sci U S A* 89, 6472–6476.

Dorfman, T., Luban, J., Goff, S. P., Haseltine, W. A. & Gottlinger, H. G. (1993). Mapping of functionally important residues of a cysteine-histidine box in the human immunodeficiency virus type 1 nucleocapsid protein. *J Virol* 67, 6159–6169.

Garzino-Demo, A., Gallo, R. C. & Arya, S. K. (1995). Human immunodeficiency virus type 2 (HIV-2): packaging signal and associated negative regulatory element. *Hum Gene Ther* 6, 177–184.

Gonsky, J., Bacharach, E. & Goff, S. P. (2001). Identification of residues of the Moloney murine leukemia virus nucleocapsid critical for viral DNA synthesis in vivo. *J Virol* 75, 2616–2626.

Gorelick, R. J., Henderson, L. E., Hanser, J. P. & Rein, A. (1988). Point mutants of Moloney murine leukemia virus that fail to package viral RNA: evidence for specific RNA recognition by a 'zinc finger-like' protein sequence. *Proc Natl Acad Sci U S A* 85, 8420–8424.

Gorelick, R. J., Nigida, S. M., Jr, Bess, J. W., Jr, Arthur, L. O., Henderson, L. E. & Rein, A. (1990). Noninfectious human immunodeficiency virus type 1 mutants deficient in genomic RNA. *J Virol* 64, 3207–3211.

Gorelick, R. J., Chabot, D. J., Rein, A., Henderson, L. E. & Arthur, L. O. (1993). The two zinc fingers in the human immunodeficiency virus type 1 nucleocapsid protein are not functionally equivalent. *J Virol* 67, 4027–4036.

Gorelick, R. J., Chabot, D. J., Ott, D. E., Gagliardi, T. D., Rein, A., Henderson, L. E. & Arthur, L. O. (1996). Genetic analysis of the zinc finger in the Moloney murine leukemia virus nucleocapsid domain: replacement of zinc-coordinating residues with other zinc-coordinating residues yields noninfectious particles containing genomic RNA. *J Virol* 70, 2593–2597.

Gorelick, R. J., Benveniste, R. E., Gagliardi, T. D. & 8 other authors (1999). Nucleocapsid protein zinc-finger mutants of simian immunodeficiency virus strain mne produce virions that are replication defective in vitro and in vivo. *Virology* 253, 259–270.

Guo, J., Henderson, L. E., Bess, J., Kane, B. & Levin, J. G. (1997). Human immunodeficiency virus type 1 nucleocapsid protein promotes efficient strand transfer and specific viral DNA synthesis

by inhibiting TAR-dependent self-priming from minus-strand strong-stop DNA. *J Virol* **71**, 5178–5188.

Guo, J., Wu, T., Anderson, J., Kane, B. F., Johnson, D. G., Gorelick, R. J., Henderson, L. E. & Levin, J. G. (2000). Zinc finger structures in the human immunodeficiency virus type 1 nucleocapsid protein facilitate efficient minus- and plus-strand transfer. *J Virol* **74**, 8980–8988.

Kaye, J. F. & Lever, A. M. (1999). Human immunodeficiency virus types 1 and 2 differ in the predominant mechanism used for selection of genomic RNA for encapsidation. *J Virol* **73**, 3023–3031.

Kestler, H., Kodama, T., Ringler, D. & 8 other authors (1990). Induction of AIDS in rhesus monkeys by molecularly cloned simian immunodeficiency virus. *Science* **248**, 1109–1112.

Komatsu, H., Tsukahara, T. & Tozawa, H. (1996). Viral RNA binding properties of human immunodeficiency virus type-2 (HIV-2) nucleocapsid protein-derived synthetic peptides. *Biochem Mol Biol Int* **38**, 1143–1154.

Kuwata, T., Igarashi, T., Ido, E., Jin, M., Mizuno, A., Chen, J. & Hayami, M. (1995). Construction of human immunodeficiency virus 1/simian immunodeficiency virus strain mac chimeric viruses having *vpr* and/or *nef* of different parental origins and their *in vitro* and *in vivo* replication. *J Gen Virol* **76**, 2181–2191.

Maurer, B., Bannert, H., Darai, G. & Flugel, R. M. (1988). Analysis of the primary structure of the long terminal repeat and the *gag* and *pol* genes of the human spumaretrovirus. *J Virol* **62**, 1590–1597.

Meric, C. & Goff, S. P. (1989). Characterization of Moloney murine leukemia virus mutants with single-amino-acid substitutions in the Cys–His box of the nucleocapsid protein. *J Virol* **63**, 1558–1568.

Meric, C., Darlix, J. L. & Spahr, P. F. (1984). It is Rous sarcoma virus protein P12 and not P19 that binds tightly to Rous sarcoma virus RNA. *J Mol Biol* **173**, 531–538.

Meric, C., Gouilloud, E. & Spahr, P. F. (1988). Mutation in Rous sarcoma virus nucleocapsid protein $P12^{NC}$: deletions of Cys–His boxes. *J Virol* **62**, 3328–3333.

Mizuno, A., Ido, E., Goto, T., Kuwata, T., Nakai, M. & Hayami, M. (1996). Mutational analysis of two zinc finger motifs in HIV type 1 nucleocapsid proteins: effects on proteolytic processing of Gag precursors and particle formation. *AIDS Res Hum Retrovir* **12**, 793–800.

Naidu, Y. M., Kestler, H. W. D., Li, Y. & 8 other authors (1988). Characterization of infectious molecular clones of simian immunodeficiency virus (SIVmac) and human immunodeficiency virus type 2: persistent infection of rhesus monkeys with molecularly cloned SIVmac. *J Virol* **62**, 4691–4696.

Prats, A. C., Sarih, L., Gabus, C., Litvak, S., Keith, G. & Darlix, J. L. (1988). Small finger protein of avian and murine retroviruses has nucleic acid annealing activity and positions the replication primer tRNA onto genomic RNA. *EMBO J* **7**, 1777–1783.

Prats, A. C., Roy, C., Wang, P. A., Erard, M., Housset, V., Gabus, C., Paoletti, C. & Darlix, J. L. (1990). Cis elements and trans-acting factors involved in dimer formation of murine leukemia virus RNA. *J Virol* **64**, 774–783.

Prats, A. C., Housset, V., De Billy, G., Cornille, F., Prats, H., Roques, B. & Darlix, J. L. (1991). Viral RNA annealing activities of the nucleocapsid protein of Moloney murine leukemia virus are zinc independent. *Nucleic Acids Res* **19**, 3533–3541.

Shibata, R., Kawamura, M., Sakai, H., Hayami, M., Ishimoto, A. & Adachi, A. (1991). Generation of a chimeric human and simian immunodeficiency virus infectious to monkey peripheral blood mononuclear cells. *J Virol* **65**, 3514–3520.

Stewart, L., Schatz, G. & Vogt, V. M. (1990). Properties of avian retrovirus particles defective in viral protease. *J Virol* **64**, 5076–5092.

Suryanarayana, K., Wiltrout, T. A., Vasquez, G. M., Hirsch, V. M. & Lifson, J. D. (1998). Plasma SIV RNA viral load determination by real-time quantification of product generation in reverse transcriptase-polymerase chain reaction. *AIDS Res Hum Retrovir* **14**, 183–189.

Tanchou, V., Decimo, D., Pechoux, C., Lener, D., Rogemond, V., Berthoux, L., Ottmann, M. & Darlix, J. L. (1998). Role of the N-terminal zinc finger of human immunodeficiency virus type 1 nucleocapsid protein in virus structure and replication. *J Virol* **72**, 4442–4447.

Urbaneja, M. A., McGrath, C. F., Kane, B. P., Henderson, L. E. & Casas-Finet, J. R. (2000). Nucleic acid binding properties of the simian immunodeficiency virus nucleocapsid protein NCp8. *J Biol Chem* **275**, 10394–10404.

Willey, R. L., Smith, D. H., Lasky, L. A., Theodorer, T. S., Earl, P. L., Mos, B., Capon, D. L. & Martin, M. A. (1988). In vitro mutagenesis identifies a region within the envelope gene of the human immunodeficiency virus that is critical for infectivity. *J Virol* **62**, 139–147.

Wu, T., Guo, J., Bess, J., Henderson, L. E. & Levin, J. G. (1999). Molecular requirements for human immunodeficiency virus type 1 plus-strand transfer: analysis in reconstituted and endogenous reverse transcription systems. *J Virol* **73**, 4794–4805.

Xiao, Y., Kuwata, T., Miura, T., Hayami, M. & Shida, H. (2000). Dox-dependent SIVmac with tetracycline-inducible promoter in the U3 promoter region. *Virology* **269**, 268–275.

You, J. C. & McHenry, C. S. (1994). Human immunodeficiency virus nucleocapsid protein accelerates strand transfer of the terminally redundant sequences involved in reverse transcription. *J Biol Chem* **269**, 31491–31495.

Yovandich, J. L., Chertova, E. N., Kane, B. P., Gagliardi, T. D., Bess, J. W., Jr, Sowder, R. C., II, Henderson, L. E. & Gorelick, R. J. (2001). Alteration of zinc-binding residues of simian immunodeficiency virus $p8^{NC}$ results in subtle differences in gag processing and virion maturation associated with degradative loss of mutant NC. *J Virol* **75**, 115–124.

Yu, Q. & Darlix, J. L. (1996). The zinc finger of nucleocapsid protein of Friend murine leukemia virus is critical for proviral DNA synthesis in vivo. *J Virol* **70**, 5791–5798.

Journal of General Virology (2003), 84, 2237–2244 DOI 10.1099/vir.0.19082-0

DNA vaccination of macaques by a full-genome simian/human immunodeficiency virus type 1 plasmid chimera that produces non-infectious virus particles

Wataru Akahata,[1] Eiji Ido,[1] Hisashi Akiyama,[1] Hiromi Uesaka,[1,3] Yoshimi Enose,[1] Reii Horiuchi,[1] Takeo Kuwata,[1] Toshiyuki Goto,[4] Hidemi Takahashi[5,2] and Masanori Hayami[1]

Correspondence
Eiji Ido
eido@virus.kyoto-u.ac.jp

[1,2]Laboratory of Viral Pathogenesis[1] and Laboratory of Viral Control[2], Institute for Virus Research, Kyoto University, Kyoto 606-8507, Japan

[3]Laboratory Animal Research Center, Toyama Medical and Pharmaceutical University, Toyama 930-0152, Japan

[4]College of Medical Technology, Kyoto University, Kyoto 606-8507, Japan

[5]Department of Microbiology and Immunology, Nippon Medical School, Tokyo 113-8602, Japan

A DNA vaccination regime was investigated previously in rhesus macaques using a full-genome human immunodeficiency virus type 1 (HIV-1) plasmid, which, due to mutations in the nucleocapsid (NC) proteins, produced only non-infectious HIV-1 particles (Akahata *et al.*, *Virology* **275**, 116–124, 2000). In that study, four monkeys were injected intramuscularly 14 times with the plasmid. All of them showed immunological responses against HIV-1 and partial protection from challenge with a simian immunodeficiency virus/HIV (SHIV) chimeric virus. To improve this DNA vaccination regime, the plasmid used for vaccination was changed. In the present study, four macaques were injected intramuscularly eight times with a full-genome SHIV plasmid that produces non-infectious SHIV particles. CTL activities were higher than those observed in monkeys vaccinated previously with the HIV-1 plasmid. In all macaques vaccinated, peak plasma virus loads after homologous challenge with SHIV were two to three orders of magnitude lower than those of the naive controls, and virus loads fell below the level of detection at 6 weeks post-challenge. This suggested that the vaccination regime in this study was partially effective and better than the previous regime.

Received 3 January 2003
Accepted 7 May 2003

INTRODUCTION

Live attenuated vaccines have been shown to be the most effective vaccine against AIDS in non-human primate models (Daniel *et al.*, 1992; Shibata *et al.*, 1997; Ui *et al.*, 1999). The main advantage of using live attenuated vaccines is that they mimic natural infection in the host. However, the safety of attenuated vaccines for human use is questionable because they have been shown to be pathogenic in neonates and possibly even in adult monkeys (Baba *et al.*, 1999).

Another candidate for an AIDS vaccine is DNA, which can elicit both humoral and cell-mediated immunity. This method consists of injection of DNA plasmids that encode antigenic proteins under a strong enhancer/promoter, such as the human cytomegalovirus immediate/early promoter.

Published ahead of print on 27 May 2003 as DOI 10.1099/vir.0.19082-0

DNA vaccines are considered to be much safer than live attenuated vaccines and initial results have been promising. Recent reports employed DNA vaccination in combination with boosting of antigenic proteins (Boyer *et al.*, 1997; Letvin *et al.*, 1997), live virus vectors (Robinson *et al.*, 1999) or cytokine augmentation (Barouch *et al.*, 2000). None of the vaccination regimes using DNA alone have achieved complete protection, which is in contrast to the rather satisfactory results obtained with live attenuated vaccines.

Previously, we reported a DNA vaccination regime using a full-genome plasmid producing non-infectious whole particles of human immunodeficiency virus type 1 strain NL432 (HIV-1_{NL432}), transcribed under its original promoter, HIV-1 LTR (Akahata *et al.*, 2000). The plasmid has mutations (Cys...Cys...His...Cys→Ser...Ser...His...Cys) in an N-terminal zinc-finger motif of the nucleocapsid protein (NC), located in the *gag* region of HIV-1. Zinc-finger motifs are believed to play an important role in packaging the viral

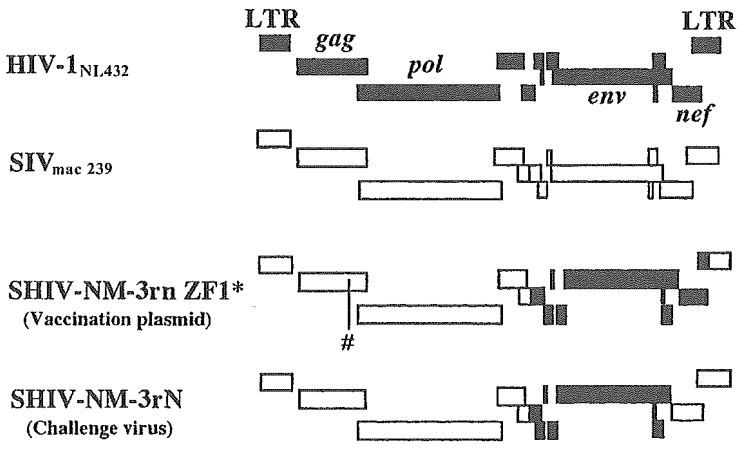

	Zinc-finger motif 1	Zinc-finger motif 2
SHIV-NM-3rn	CWNCGKEGHSARQC	CWKCGKMDHVMAKC
SHIV-NM-3rn ZF1*	SWNSGKEGHSARQC	CWKCGKMDHVMAKC

Fig. 1. Genetic structure of HIV-1_{NL432}, SIV_{mac239}, SHIV-NM-3rn, zinc-finger mutant SHIV-NM-3rn ZF1* and a challenge virus, SHIV-NM-3rN. Solid and open boxes represent sequences derived from HIV-1_{NL432} and SIV_{mac239}, respectively. '#', Mutated amino acids in SHIV-NM-3rn ZF1* zinc-finger motifs present in the NC. Mutated amino acid residues are underlined.

genomic RNA. The mutant plasmid expresses whole virus component proteins to produce virus particles that do not possess genomic RNA (Mizuno *et al.*, 1996). All monkeys that had been injected intramuscularly with the plasmid 14 times showed immunological responses against HIV-1: stable anti-HIV-1 Env antibodies were raised in two monkeys and CTL activity against HIV-1 was induced in the other monkeys. All monkeys showed partial protection against challenge with 100 $TCID_{50}$ of a simian immunodeficiency virus/HIV chimeric virus (SHIV), termed SHIV-NM-3rN (Kuwata *et al.*, 1995). Namely, peak plasma virus loads of the challenge virus were two to three orders of magnitude lower than they were in naive controls. However, we repeated the DNA injections a total of 14 times because of the inefficient expression of the proteins encoded by the plasmid.

To improve the DNA vaccination regime described previously, we vaccinated animals with a novel SHIV plasmid, termed pSHIV-NM-3rn ZF1*. The mutant plasmid pSHIV-NM-3rn ZF1* produces non-infectious SHIV whole virus particles similar to those produced by pNL432 ZF1* due to the mutation in the NC proteins. We expected that the expression of pSHIV-NM-3rn ZF1*, which is driven by the SIV LTR promoter, might be better in monkeys than the expression of pNL432 ZF1*, which is driven by the HIV-1 LTR promoter.

An advantage of a full-genome plasmid is that it is capable of expressing all of the viral antigenic components, including the Gag, Pol and Env proteins. Recently, some reports suggested that a single viral epitope-specific CTL response may not be sufficient to block infection with pathogenic SIV (Hanke *et al.*, 1999; Yasutomi *et al.*, 1995). Our DNA vaccine included all viral epitopes. In addition, this regime more closely resembles the use of a live attenuated vaccine than the foregoing DNA vaccination regimes. Live attenuated vaccines replicate in infected cells and viral antigenic components are presented by way of MHC molecules on the infected cell surface, thus eliciting a strong immunity against the virus in the host. Viral genes contained in the full-genome plasmid are expected to be expressed in a similar manner, leading to the assembly of virus components and budding of virus particles in the cells that took up the plasmid. This series of events is believed to be effective for acquisition of cellular and humoral immunity in the host.

METHODS

Plasmid for DNA vaccination. An infectious molecular clone of SHIV-NM-3rn (Kuwata *et al.*, 1995) was used as a parent proviral DNA in this study (Fig. 1). The *Bam*HI–*Pvu*II fragment (nt 2106–2705), which includes a part of the *gag* open reading frame, was subcloned between the *Bam*HI/*Hin*cII sites of pUC119 and, using this plasmid as a template, site-directed mutagenesis of the zinc-finger motifs was performed by PCR (Fig. 2).

To generate the first finger-motif mutant (designated SHIV-NM-3rn ZF1*), in which the first two cysteine residues in the motif were replaced by serine residues, PCR was performed using the oligonucleotide 5′-TGGGGCTCTGCATTGCCTTGCAGAGTGTCCCTCTT-TCCCAGAATTCCAAGACTTAATTGGC-3′ (nt 2535–2475) as a reverse primer and the F13 universal primer as a forward primer. The former oligonucleotide was designed to create an *Eco*RI site (indicated in boldface) in addition to alterating specific nucleotides (underlined). The product amplified by PCR was electrophoretically separated on an agarose gel and purified using the Geneclean II kit (BIO 101). The fragment was then digested with *Bam*HI (nt 2106) and *Ban*II (nt 2533). Another fragment obtained from the above-mentioned plasmid pUC119 harbouring the *Bam*HI–*Pvu*II fragment of SHIV-NM-3rN (nt 2106–2705) was also digested with *Ban*II/*Pvu*II. These two fragments, *Bam*HI–*Ban*II (nt 2106–2533) and *Ban*II–*Pvu*II (nt 2533–2705), were subcloned as a consecutive form between the *Bam*HI site and the *Hin*cII site of pUC119. The plasmid generated was then digested with *Bam*HI/*Ppu*MI (nt 2698). The *Bam*HI–*Ppu*MI fragment obtained was reinserted into the corresponding position in the pUC119 plasmid harbouring the *Bam*HI–*Sse*8387I fragment of

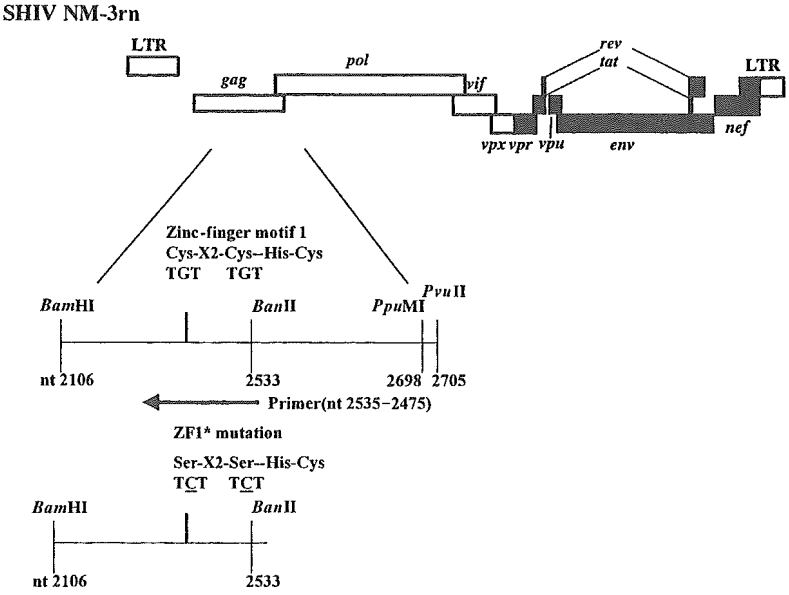

Fig. 2. Construction of SHIV-NM-3rn ZF1*. An infectious molecular clone of SHIV-NM-3rn was used as the parent proviral DNA. The *Bam*HI–*Pvu*II fragment was subcloned into pUC119 and, using this plasmid as a template, site-directed mutagenesis of the zinc-finger motif was performed by PCR. The PCR fragment with the Ser...Ser...His...Cys mutations in zinc-finger motif 1 was then digested with *Bam*HI/*Ban*II and was reinserted into the corresponding position in pSHIV-NM-3rn, as described in Methods.

SHIV-NM-3rn (nt 2105–3402). The plasmid generated was then digested with *Bam*HI/*Sse*8387I and the *Bam*HI–*Sse*8387I fragment (nt 2105–3402) obtained was reinserted into the corresponding position in pSHIV-NM-3rn (Kuwata *et al.*, 1995).

Cell culture and transfections. COS-1 cells were cultured in DMEM containing 10% heat-inactivated FBS (Gibco-BRL) and 20 mM L-glutamine. M8166 cells (a human $CD4^+$ lymphoid cell line) were cultured in RPMI 1640 medium containing 10% FBS and 20 mM L-glutamine. Cells were transfected using the FuGENE-6 Transfection Reagent kit (Roche) with 20 μg of the viral plasmid DNAs, following the manufacturer's recommendations.

Reverse transcriptase (RT) assay and ELISA. The RT assay was performed as described (Mizuno *et al.*, 1996). The amount of $p27^{CA}$ in the culture supernatant was measured using the SIV Core Antigen ELISA kit (Coulter).

Quantitative RT-PCR. To measure the genomic RNA in virus particles, we performed quantitative RT-PCR as follows. The transfected culture supernatant was filtered through a 0·45 μm pore-size filter and viral RNA was extracted using the QIAamp Viral RNA Mini kit (Qiagen). To remove contaminating plasmid DNA, the precipitated RNA was digested with DNase I (Gibco-BRL) for 15 min at 37 °C, followed by heat treatment (15 min at 70 °C) to inactivate the DNase I. RT reactions and subsequent PCR conditions were performed using the Taqman RT-PCR kit (Perkin Elmer), according to the manufacture's recommendations. SIVII-696F (5′-GGAAATTACCCAGTACAACAAATAGG-3′) and SIVII-784R (5′-TCTATCAATTTTACCCAGGACTTTA-3′) were used as primers, and a labelling probe, SIVII-731 (5′-Fam-TGTCCACCTGCCATTAAGCCCG-Tamra-3′) (Perkin Elmer), was also used.

Immunoblot analysis. Immunoblot analysis was performed as described (Mizuno *et al.*, 1996). In brief, for an immunoblot analysis of transfected cells, the cells were washed three times and, at 3 days after transfection, were lysed in lysis buffer and subjected to analysis. Plasma from a SHIV-NM-3rN-infected monkey (Kuwata *et al.*, 1995) was used to provide the first antibody. To analyse for virus particles, the transfected culture supernatant was filtered through a 0·45 μm pore-size filter. Each sample was adjusted to contain an equal amount of RT activity in the supernatant. The virus particles released were pelleted by centrifugation at 14 000 r.p.m. for 2 h at 4 °C. The pelleted virions were then lysed in lysis buffer and subjected to immunoblot analysis.

Electron microscopy. The morphology of the virus particles produced by full-genome plasmids was examined under electron microscopy. Transfected COS-1 cells were prefixed for 2 h in 2% glutaraldehyde in PBS and washed thoroughly with PBS. The cells were then fixed with 1% osmium tetroxide in PBS, dehydrated and embedded in epoxy resin. Ultrathin sections of the cells were stained with uranyl acetate and lead citrate and then observed under a Hitachi H-7100 electron microscope, as described (Mizuno *et al.*, 1996).

Vaccination protocol. Plasmids were amplified in *Escherichia coli* on a large scale and extracted from the cells by conventional alkaline lysis methodology followed by purification with ethanol and polyethylene glycol precipitation. Four mature male rhesus macaques (*Macaca mulatta*) (MM212, MM214, MM231 and MM234) were injected intramuscularly at two points on the right quadriceps and at two points on the calves with a solution containing 500 μg pSHIV-NM-3rn ZF1* in 450 μl PBS and 450 μl bupivacaine (Fujisawa Pharmaceutical) per injection for a total of eight injections. We injected the plasmid in two sets of DNA immunization series. Each set comprised one injection per week for four consecutive weeks. We injected at 0–3 weeks post initial vaccination (p.v.) and, after an interval of 5 weeks, we gave the second set of DNA immunizations, at 10–13 p.v.

Animals. All macaques used in this study were serologically negative for SIV and simian T cell lymphotropic virus type 1 before vaccination. They were housed throughout the experimental period and autopsies were carried out in accordance with regulations approved by the Institutional Animal Care and Use Committee of the Institute for Virus Research, Kyoto University, Japan.

Assays for antibodies. The titres of anti-Env antibodies in the plasma of the monkeys vaccinated were determined using the Genscreen HIV-1/2 kit (Fujirebio), following the manufacturer's recommendations. The kit is based on a sandwich ELISA and the wells of microtitre plates were coated with the recombinant proteins HIV-1 gp160 p25, and synthetic peptides HIV-1 gp41 and HIV-2 gp36.

Particle agglutination was measured using the Serodia HIV-1/2 kit

(Serodia HIV, Fujirebio) and immunoblotting was measured using the LAV BLOT 1 and LAV BLOT 2 kits (LAV BLOT, Fujirebio), following the manufacturer's recommendations. The LAV BLOT 1 kit was used for detection of HIV-1 Env antibodies and the LAV BLOT 2 kit was used for detection of SIV Gag antibodies.

Assay for HIV-1 Env- and SIV Gag-specific killer cell activities. Specific killer cell activities for HIV-1 Env and SIV Gag were measured as described previously (Akahata *et al.*, 2000; Yamamoto *et al.*, 1990). Herpesvirus papio-transformed B lymphocyte cell lines (B-LCL) established from the respective monkey PBMCs were infected with an HIV-1 Env (HIV-1_{IIIb}) or SIV Gag (SIV_{mac239})-expressing recombinant vaccinia virus and used as target cells. The parental vaccinia virus-infected and non-infected cells were used as control targets. HIV-1 Env- and SIV Gag-specific killer cell activities were expressed as the percentage of specific lysis: (% specific lysis) = (% lysis of the HIV-1 Env- or SIV Gag-expressing B-LCL) − (% lysis of the parental vaccinia virus-infected B-LCL), when the effector : target cell ratio was 50 : 1. (In some cases, slightly lower ratios were adopted due to a limited number of the available cells.) The respective monkey B-LCLs infected with HIV-1 Env- or SIV Gag-expressing vaccinia virus were killed by treatment with glutaraldehyde and were used as antigen-stimulator cells. The respective monkey PBMCs were stimulated by the HIV-1 Env- or SIV Gag-expressing B-LCLs and incubated for 5 days. Stimulated PBMCs were used as the effector cells. The values of per cent specific lysis were measured in triplicate and mean values are shown. A per cent specific lysis value of above 7·0 was considered as 'specific killer activity'. HIV-1 Env- and SIV Gag-specific killer cell activities were measured in MM212 and MM214 at 16 and 24 weeks p.v. and in MM231 and MM234 at 14 and 19 weeks p.v., respectively.

Lymphocyte proliferation assay. PBMCs were obtained from the vaccinated monkeys and cultured in a 96-well plate (2×10^5 cells per well) in 200 µl RPMI in the presence of 2·5 µg HIV-1 rgp160 ml^{-1} (HIV-1_{IIIB} gp160 recombinant viral protein) (Advanced Biotechnologies) for 72 h. Then lymphocyte proliferation was measured using a cell proliferation ELISA kit (Roche Diagnostics), following the manufacturer's recommendations. The ratio of incorporated BrdU by PBMCs for 24 h in the presence of antigen to that in media alone was expressed as the stimulation index (SI). An SI value above 2·5 was considered as 'antigen-specific stimulation'. As a positive control, PBMCs were cultured in the presence of 1 µg concanavalin A (ConA) as a polyclonal stimulator. ConA-stimulated proliferation was found and the SI values were above 5·0 in all assays.

Challenge virus. SHIV-NM-3rN was used as a challenge virus, in which the *env*, *rev*, *tat*, *vpu* and *vpr* genes are derived from HIV-1_{NL432} and the rest of the genome is derived from SIV_{mac239} (Kuwata *et al.*, 1995). NM-3rN possesses identical genes, except for the *nef* gene, to the one in the vaccinated plasmid (Fig. 1). SHIV-NM-3rN was grown in macaque monkey PBMCs and cell-free virus stocks were prepared. Four vaccinated macaques and two naive macaques were challenged intravenously with 1×10^2 $TCID_{50}$ SHIV-NM-3rN.

Detection of plasma viral RNA. Plasma virus loads were determined after challenge. Viral RNA was extracted from the plasma using the QIAamp Viral RNA Mini kit and their levels were determined by quantitative RT-PCR using a Taqman RT-PCR kit (Suryanarayana *et al.*, 1998). Primers used in this assay were SIVII-696F and SIVII-784R and the probe was SIVII-731 (Perkin-Elmer). For a standard curve, quantitative assays for the measurement of viral RNA copy numbers in plasmas of a SHIV-infected monkey were performed by the Bayer Reference Testing Laboratory (Emeryville) with a branched DNA Signal Amplification assay (Pachl *et al.*, 1995; Tsai *et al.*, 1997). For each run, a standard curve was generated from dilutions of viral RNA extracted from the monkey's plasma. Under these conditions, the detection limit was 500 copies ml^{-1}.

Virus isolation. Virus was isolated as described previously (Ui *et al.*, 1999). In brief, PBMCs were obtained from the monkeys at 2 and 4 weeks post-challenge (p.c.). Then, 1×10^6 PBMCs were co-cultured with 1×10^6 M8166 cells for 4 weeks in RPMI 1640 medium supplemented with 10 % FBS and 20 mM L-glutamine.

Detection of recombination. DNA was extracted using the QIAamp DNA Mini kit. PCR was carried out using extracted DNA from 5×10^4 cells and the primer pair HnefF1 (5′-ACAGGGCTTGGAAAGGATTTTGCTA-3′, nt 9350–9374) and SnefR1 (5′-CCCCGTAACATCCCCTTGTGGAAAGTCCC-3′, nt 10178–10206). The challenge virus, SHIV-NM-3rN, was detected as a 859 bp band and the vaccination plasmid, pSHIV-NM-3rn ZF1*, was detected as a 680 bp band. To determine whether the vaccination plasmid (which has an *Xho*I site) was present, the PCR products were incubated with *Xho*I. Cleavage at this site would create bands of 580 and 100 bp in size. The regions of the challenge viruses amplified do not have an *Xho*I site. Thus, if the PCR products were not digested with *Xho*I, then they would have been derived only from the challenge virus.

RESULTS

Vaccinated plasmid

We used the plasmid pSHIV-NM-3rn ZF1* for DNA vaccination (Fig. 1). The plasmid is derived from an infectious molecular clone SHIV-NM-3rn (Kuwata *et al.*, 1995), which is a SHIV comprising LTR, *gag*, *pol*, *vif* and *vpx* from SIV_{mac239} (Kestler *et al.*, 1990) and *vpr*, *tat*, *rev*, *vpu*, *env* and *nef* from HIV-1_{NL432} (Adachi *et al.*, 1986). The plasmid pSHIV-NM-3rn ZF1* has mutations (Cys...Cys...His...Cys→Ser...Ser...His...Cys) in an N-terminal zinc-finger motif of the NC protein in the *gag* region of SHIV-NM-3rn.

Zinc-finger mutants of HIV-1 and Moloney murine leukaemia virus have been reported to be non-infectious (Gorelick *et al.*, 1990; Meric & Goff, 1989; Mizuno *et al.*, 1996). We next determined whether the pSHIV-NM-3rn ZF1* plasmid produced infectious virus. $CD4^+$ M8166 cells were infected with the supernatants of transfected COS-1 cells containing equal amounts of viral RNAs, as measured by quantitative RT-PCR. Conspicuous syncytium formation was observed in M8166 cells infected with the supernatant from the SHIV-NM-3rn plasmid. The culture supernatant of these cells accumulated RT activity. In contrast, there was no indication of infectivity in the cells infected with the supernatants from pSHIV-NM-3rn ZF1* during the observation period of more than 1 month. Thus, the alteration in the N-terminal zinc finger resulted in the total loss of virus infectivity.

Virus particles produced by the mutant DNA had almost the same amount of $p27^{CA}$, $p17^{MA}$ and unprocessed Gag precursor proteins as the wild-type. An immunoblot analysis together with electron microscopic observation showed that the plasmid pSHIV-NM-3rn ZF1* produced non-infectious virus particles with an average diameter of

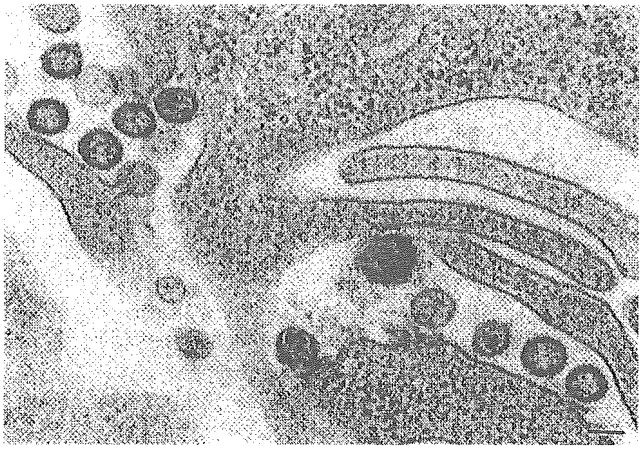

Fig. 3. An electron micrograph of the virus particles produced by a zinc-finger mutant plasmid pSHIV-NM-3rn ZF1*. COS-1 cells transfected with the mutant plasmid were harvested at 48 h after transfection and subjected to electron microscopic observation. Bar, 100 nm.

100 nm (Fig. 3). Similar results were obtained using pSHIV-NM-3rn (data not shown).

Antibody response in DNA-vaccinated macaques

Four macaques (MM212, MM214, MM231 and MM234) were vaccinated using a DNA vaccination regime with the SHIV full-genome plasmid, pSHIV-NM-3rn ZF1*. The vaccination schedule is shown in Fig. 4.

None of the monkeys showed an antibody response against HIV-1 Env up until 24 weeks p.v., as measured by ELISA. Antibody titres against HIV-1/2 were also measured by particle agglutination, which gave results that were the same as those obtained by ELISA. No detectable anti-HIV-1/2 antibodies were observed up until the day of challenge. We also employed an immunoblotting assay to see any antibody response, but the sera of all of the vaccinated monkeys at 8, 14, 16 and 24 weeks p.v. did not show any specific antibody by an HIV-2 Western blot kit that can detect anti-SIV Gag antibodies.

HIV-1 Env- and Gag-specific killer cell activities

Table 1 summarizes HIV-1 Env- and Gag-specific killer cell activities in the monkeys between 14 and 24 weeks p.v. All monkeys vaccinated showed HIV-1 Env- or SIV Gag-specific killer cell activities. MM234 showed HIV-1 Env- and SIV Gag-specific killer cell activities at 14 weeks p.v. (against Env at 14 and 19 weeks p.v. and against Gag at 14 weeks p.v.). MM212, MM214 and MM231 showed Gag-specific killer cell activities at 24 weeks p.v., at 16 and 24 weeks p.v. and at 19 weeks p.v., respectively.

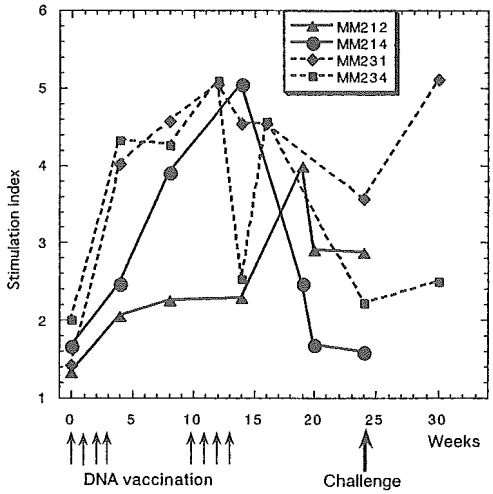

Fig. 4. Lymphocyte proliferation against HIV-1 Env in monkeys immunized with pSHIV-NM-3rn ZF1*, as measured by a cell proliferation ELISA kit. Arrows indicate the times of DNA vaccination. The arrow in bold indicates the time of challenge with SHIV-NM-3rN.

Lymphocyte proliferation

Lymphocyte proliferation was measured by determining the ratio of incorporated BrdU by PBMCs in the presence of HIV-1 rgp160. SI values increased in all monkeys vaccinated, indicating the presence of antigen-specific helper T cell lymphocyte memory (Fig. 4). SI values in all monkeys before vaccination were below 2. However, values increased to above 3 after the eighth injection in MM212 and after the fourth injection in the other three monkeys.

Table 1. HIV-1 Env- or SIV Gag-specific killer cell activities in macaques vaccinated with DNA

An effector to target (E:T) cell ratio of 50:1 was used unless indicated otherwise. Ratios were changed due to experimental conditions.

Monkey	Weeks p.v.	% specific lysis	
		HIV-1 Env	SIV Gag
MM212	16	3·4	2·6
MM214	16	3·5	9·6†
MM231	14	6·3	5·9
MM234	14	7·0*	8·3
MM212	24	ND	8·7
MM214	24	ND	18·5
MM231	19	0	17·6
MM234	19	7·2	0

*E:T ratio of 30:1.
†E:T ratio of 25:1.
ND, Not done.

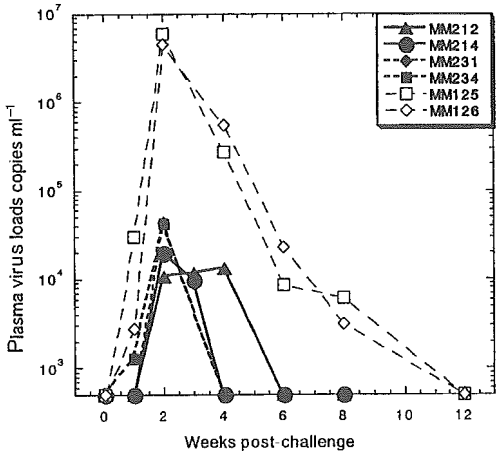

Fig. 5. Plasma virus loads of vaccinated and naive control macaques after challenge with SHIV-NM-3rN. Plasma virus loads were measured by RT-PCR. Vaccinated monkeys: MM212, MM214, MM231 and MM234; naive monkeys, MM125 and MM126.

Virus loads of challenge virus in plasma

Vaccinated monkeys were intravenously challenged with a 100 $TCID_{50}$ dose of SHIV-NM-3rN at 24 weeks p.v. Two naive macaques, MM125 and MM126, were also inoculated as unvaccinated controls.

Plasma virus loads were monitored by quantitative RT-PCR (Fig. 5). Viral RNA was not detected in any of the macaque sera before challenge with the infectious virus. Virus loads in the two naive monkeys (MM126 and MM125) at 1 week p.c. were approximately $2{\cdot}7 \times 10^3$ and 3×10^4 copies ml^{-1}, respectively. Then, at 2 weeks p.c., the virus loads of these two monkeys reached their peak values (both approximately 10^7 copies ml^{-1}). The virus loads of these monkeys remained above the detection limit until 12 weeks p.c. On the other hand, at 1 week p.c., the virus load of MM234 was below $1{\cdot}5 \times 10^3$ copies ml^{-1} and the virus loads of the other vaccinated monkeys were below the detectable level. Peak virus loads at 2 weeks p.c. of all vaccinated monkeys were two to three orders of magnitude lower than those of the naives. It is noteworthy that it took only 4 weeks for the virus loads to decrease below the detectable level in the three monkeys vaccinated.

Detection of recombination between the vaccinated plasmid and the challenge virus

No infectious virus was recovered from MM214, MM231 or MM234 at 2 and 4 weeks p.c., while infectious virus was recovered from MM212, but only at 2 weeks p.c. The *nef* region of the virus recovered from MM212 was amplified by PCR. It was found that the PCR product was not cut by *Xho*I. Since only the vaccination plasmid has an *Xho*I site, this indicated that only the challenge virus was present, suggesting that there was no recombination between the vaccination plasmid and the challenge virus. Although we extracted the PBMCs of the other animals and screened for recombination events, we could not amplify the proviral DNA from the stored, frozen PBMCs, probably due to the very low copy numbers of the proviral DNA.

DISCUSSION

In a previous study, we injected four monkeys 14 times with the HIV-1 plasmid pNL432 ZF1* (Akahata *et al.*, 2000). In this study, we injected four monkeys with the plasmid pSHIV-NM-3rn ZF1*, expecting that the expression of this plasmid, which is driven by the SIV LTR promoter, would be better than that of the pNL432 ZF1*, which is driven by the HIV-1 LTR promoter, in monkeys. This is because HIV-1 has a narrow host range and cannot infect non-human primates such as rhesus macaques (*Macaca mulatta*). Although the determinants of macaque cell tropism are unknown, a SHIV comprising LTR and *gag* from SIV_{mac239} and *env* from HIV-1 can infect macaques but a SHIV comprising LTR and *gag* from HIV-1 and *env* from SIV_{mac239} cannot (Shibata *et al.*, 1991). In this study, none of the monkeys vaccinated showed any anti-HIV-1 Env antibodies, three of the monkeys showed no anti-SIV Gag antibodies and the fourth had only weak anti-SIV Gag antibodies. On the other hand, two of the monkeys vaccinated in the previous study (Akahata *et al.*, 2000) showed anti-HIV-1 Env and Gag antibodies. In this regard, the pSHIV-NM-3rn ZF1* plasmid did not achieve higher expression than the previous plasmid. However, all monkeys vaccinated in the present study showed CTL responses, while only two of four monkeys vaccinated in the previous study showed CTL responses. In addition, CTL responses in the previous study were lower than those in the present study. These observations might be due to the higher expression achieved by the SIV LTR promoter. The challenge virus was given at the same dose that SHIV-NM-3rN was given in the previous study. After challenge with SHIV-NM-3rN, peak plasma virus loads were two to three orders of magnitude lower than those of the naive control monkeys in the present and previous study. However, the viral RNA load in all monkeys vaccinated in the present study was lower. The viral RNA load was detected in only one monkey at 4 weeks p.c. and it was not detected in any of the monkeys at 6 weeks p.c. and thereafter. On the other hand, in the previous study, the virus was detected for a longer period; it was present in two monkeys at 4 and 6 weeks p.c., even though the injections were much more frequent than those in the present study. Overall, these results suggested that the vaccination plasmid pSHIV-NM-3rn ZF1* was better than plasmid pNL432 ZF1* in monkeys.

Recently, some studies have reported DNA vaccination regimes that use a replication-defective full-genome plasmid for cats or non-human primates. The cats vaccinated with a full-genome plasmid showed a CTL response but did not show any antibody response (Hosie *et al.*, 1998). In the 11 monkeys vaccinated with the full SIV genome, only three

monkeys showed antibody responses (Gorelick *et al.*, 2000). Our previous report (Akahata *et al.*, 2000) showed that two of four monkeys vaccinated with the full genome of HIV-1_{NL432} had antibody responses. In the present study, all monkeys vaccinated showed a CTL response. However, three monkeys did not show any antibody response and one monkey showed only a weak anti-Gag antibody response. These recent studies (Hosie *et al.*, 1998; Gorelick *et al.*, 2000; Akahata *et al.*, 2000) reported that vaccinations that induced little or no antibody response still conferred moderate protection against challenge viruses. It seemed to be more important to induce a CTL response than an antibody response. DNA vaccinations with a full-genome plasmid tend to induce cell-mediated immunity but also tend to be not so effective at inducing humoral immunity during the period soon after the vaccination. Overexposure to the antigens may shift the immunity from a Th1-type immunity to a Th2-type immunity (Fuller & Haynes, 1994; Haynes *et al.*, 1994). The difficulty of inducing antibody responses with the full-genome DNA vaccination could be due to insufficient antigen expression shifting to Th2-type immunity, as we suggested previously (Akahata *et al.*, 2000).

There is some reluctance to use full-genome plasmids as vaccines because of the possibility of the genome reverting to the pathogenic wild-type. When we designed the plasmid pSHIV-NM-3rn ZF1*, we changed 4 nt to alter two cysteine residues to two serine residues in an N-terminal zinc-finger motif to reduce the possibility of reversion. Thus, reversion to the wild-type seems very unlikely. To confirm the safety of our vaccination regime, we examined the recombination between the DNA vaccination plasmids and the challenge viruses. No other studies have yet reported a recombination between a DNA vaccination plasmid and a challenge virus. In the present study, no recombination was observed.

In this study, we showed that a DNA vaccination regime using a full-genome plasmid was potentially effective without acting in combination with any other booster. Further studies are needed to determine whether modification of this regime, such as by using the plasmid in combination with protein or recombinant virus vector boosters, can achieve better protection.

ACKNOWLEDGEMENTS

We are grateful to Takami Tukiyama for technical assistance. This work was supported by a Health Sciences Research Grant from the Ministry of Health, Labour and Welfare, Japan, a Grant-in-Aid for Scientific Research from the Ministry of Education and Science, Japan and a Research Grant on Health Sciences focusing on Drug Innovation from the Japan Health Sciences Foundation.

REFERENCES

Akahata, W., Ido, E., Shimada, T. & 7 other authors (2000). DNA vaccination of macaques by a full genome HIV-1 plasmid which produces noninfectious virus particles. *Virology* 275, 116–124.

Alter, H. J., Eichberg, J. W., Masur, H., Saxinger, W. C., Gallo, R., Macher, A. M., Lane, H. C. & Fauci, A. S. (1984). Transmission of HTLV-III infection from human plasma to chimpanzees: an animal model for AIDS. *Science* 226, 549–552.

Baba, T. W., Liska, V., Khimani, A. H. & 8 other authors (1999). Live attenuated, multiply deleted simian immunodeficiency virus causes AIDS in infant and adult macaques. *Nat Med* 5, 194–203.

Barouch, D. H., Santra, S., Schmitz, J. E. & 26 other authors (2000). Control of viremia and prevention of clinical AIDS in rhesus monkeys by cytokine-augmented DNA vaccination. *Science* 290, 486–492.

Boyer, J. D., Ugen, K. E., Wang, B. & 12 other authors (1997). Protection of chimpanzees from high-dose heterologous HIV-1 challenge by DNA vaccination. *Nat Med* 3, 526–532.

Daniel, M. D., Kirchhoff, F., Czajak, S. C., Sehgal, P. K. & Desrosiers, R. C. (1992). Protective effects of a live attenuated SIV vaccine with a deletion in the *nef* gene. *Science* 258, 1938–1941.

Fuller, D. H. & Haynes, J. R. (1994). A qualitative progression in HIV type 1 glycoprotein 120-specific cytotoxic cellular and humoral immune responses in mice receiving a DNA-based glycoprotein 120 vaccine. *AIDS Res Hum Retroviruses* 10, 1433–1441.

Gorelick, R. J., Nigida, S. M., Jr, Bess, J. W., Jr, Arthur, L. O., Henderson, L. E. & Rein, A. (1990). Noninfectious human immunodeficiency virus type 1 mutants deficient in genomic RNA. *J Virol* 64, 3207–3211.

Gorelick, R. J., Benveniste, R. E., Lifson, J. D. & 10 other authors (2000). Protection of *Macaca nemestrina* from disease following pathogenic simian immunodeficiency virus (SIV) challenge: utilization of SIV nucleocapsid mutant DNA vaccines with and without an SIV protein boost. *J Virol* 74, 11935–11949.

Hanke, T., Samuel, R. V., Blanchard, T. J. & 9 other authors (1999). Effective induction of simian immunodeficiency virus-specific cytotoxic T lymphocytes in macaques by using a multiepitope gene and DNA prime-modified vaccinia virus Ankara boost vaccination regimen. *J Virol* 73, 7524–7532.

Haynes, J. R., Fuller, D. H., Eisenbraun, M. D., Ford, M. J. & Pertmer, T. M. (1994). Accell particle-mediated DNA immunization elicits humoral, cytotoxic, and protective immune responses. *AIDS Res Hum Retroviruses* 10, S43–S45.

Hosie, M. J., Flynn, J. N., Rigby, M. A. & 9 other authors (1998). DNA vaccination affords significant protection against feline immunodeficiency virus infection without inducing detectable antiviral antibodies. *J Virol* 72, 7310–7319.

Kestler, H., Kodama, T., Ringler, D. & other authors (1990). Induction of AIDS in rhesus monkeys by molecularly cloned simian immunodeficiency virus. *Science* 248, 1109–1112.

Kuwata, T., Igarashi, T., Ido, E., Jin, M., Mizuno, A., Chen, J. & Hayami, M. (1995). Construction of human immunodeficiency virus 1/simian immunodeficiency virus strain mac chimeric viruses having *vpr* and/or *nef* of different parental origins and their *in vitro* and *in vivo* replication. *J Gen Virol* 76, 2181–2191.

Letvin, N. L., Montefiori, D. C., Yasutomi, Y. & 9 other authors (1997). Potent, protective anti-HIV immune responses generated by bimodal HIV envelope DNA plus protein vaccination. *Proc Natl Acad Sci U S A* 94, 9378–9383.

Meric, C. & Goff, S. P. (1989). Characterization of Moloney murine leukemia virus mutants with single-amino-acid substitutions in the Cys-His box of the nucleocapsid protein. *J Virol* 63, 1558–1568.

Mizuno, A., Ido, E., Goto, T., Kuwata, T., Nakai, M. & Hayami, M. (1996). Mutational analysis of two zinc-finger motifs in HIV type 1 nucleocapsid proteins: effects on proteolytic processing of Gag precursors and particle formation. *AIDS Res Hum Retroviruses* 12, 793–800.

Pachl, C., Todd, J. A., Kern, D. G. & other authors (1995). Rapid and precise quantification of HIV-1 RNA in plasma using a branched DNA signal amplification assay. *J Acquir Immune Defic Syndr Hum Retrovirol* **8**, 446–454.

Robinson, H. L., Montefiori, D. C., Johnson, R. P. & 14 other authors (1999). Neutralizing antibody-independent containment of immunodeficiency virus challenges by DNA priming and recombinant pox virus booster immunizations. *Nat Med* 5, 526–534.

Shibata, R., Kawamura, M., Sakai, H., Hayami, M., Ishimoto, A. & Adachi, A. (1991). Generation of a chimeric human and simian immunodeficiency virus infectious to monkey peripheral blood mononuclear cells. *J Virol* **65**, 3514–3520.

Shibata, R., Siemon, C., Czajak, S. C., Desrosiers, R. C. & Martin, M. A. (1997). Live, attenuated simian immunodeficiency virus vaccines elicit potent resistance against a challenge with a human immunodeficiency virus type 1 chimeric virus. *J Virol* **71**, 8141–8148.

Suryanarayana, K., Wiltrout, T. A., Vasquez, G. M., Hirsch, V. M. & Lifson, J. D. (1998). Plasma SIV RNA viral load determination by real-time quantification of product generation in reverse transcriptase-polymerase chain reaction. *AIDS Res Hum Retroviruses* **14**, 183–189.

Tsai, C. C., Follis, K. E., Beck, T. W., Sabo, A., Bischofberger, N. & Dailey, P. J. (1997). Effects of R-9-(2-phosphonylmethoxypropyl) adenine monotherapy on chronic SIV infection in macaques. *AIDS Res Hum Retroviruses* **13**, 707–712.

Ui, M., Kuwata, T., Igarashi, T. & 9 other authors (1999). Protection of macaques against a SHIV with a homologous HIV-1 Env and a pathogenic SHIV-89.6P with a heterologous Env by vaccination with multiple gene-deleted SHIVs. *Virology* **265**, 252–263.

Yamamoto, H., Miller, M. D., Watkins, D. I., Snyder, G. B., Chase, N. E., Mazzara, G. P., Gritz, L., Panicali, D. L. & Letvin, N. L. (1990). Two distinct lymphocyte populations mediate simian immunodeficiency virus envelope-specific target cell lysis. *J Immunol* **145**, 3740–3746.

Yasutomi, Y., Koenig, S., Woods, R. M. & other authors (1995). A vaccine-elicited, single viral epitope-specific cytotoxic T lymphocyte response does not protect against intravenous, cell-free simian immunodeficiency virus challenge. *J Virol* **69**, 2279–2284.

ACADEMIC PRESS

Available online at www.sciencedirect.com

SCIENCE DIRECT®

VIROLOGY

Virology 306 (2003) 334–346

www.elsevier.com/locate/yviro

Comparative histopathological studies in the early stages of acute pathogenic and nonpathogenic SHIV-infected lymphoid organs

Toshihide Shimada,[a] Hajime Suzuki,[b] Makiko Motohara,[b] Takeo Kuwata,[b] Kentaro Ibuki,[b] Masahiro Ui,[b] Tohko Iida,[c] Manabu Fukumoto,[d,1] Tomoyuki Miura,[b,*] and Masanori Hayami[b]

[a] *Department of Pathology, Kyoto City Hospital, Kyoto 604-8845, Japan*
[b] *Institute for Virus Research, Kyoto University, Sakyo-ku Kyoto 606-8507, Japan*
[c] *Department of Microbiology, Kyoto Prefectural University of Medicine, Kyoto 602-8566, Japan*
[d] *Department of Pathology and Biology of Diseases, Graduate School of Medicine, Kyoto University, Kyoto 606-8507, Japan*

Received 8 February 2002; returned to author for revision 1 July 2002; accepted 18 July 2002

Abstract

To clarify the early pathological events in simian and human immunodeficiency chimeric virus (SHIV)-infected lymphoid organs, we examined rhesus macaques infected with an acute pathogenic SHIV (SHIV89.6P) or a nonpathogenic SHIV (NM-3rN) by sequential biopsies and serial necropsies. In the SHIV89.6P-infected monkeys, acute thymic involution as shown by increased cortical tingible-body macrophages and by neutrophilic infiltrates without follicular aggregation in the medulla began within 14 days postinoculation (dpi). Cells that were strongly positive for the virus were identified in the thymic medulla. SHIV89.6P-infected lymph nodes showed severe paracortical lymphadenitis with scattered virus-positive cells at 14 dpi and they developed paracortical depletion without the obvious follicular involution. In contrast, NM-3rN-infected monkeys showed no signs of thymic dysinvolution and the lymph nodes exhibited only follicular hyperplasia. NM-3rN-infected monkeys showed much fewer virus-positive cells in these lymphoid tissues than did SHIV89.6P-infected monkeys during the same period. These differences clearly reflect the difference in the virulence of these SHIVs.

Keywords: AIDS; HIV; SIV; Animal model; Rhesus monkey; Pathology

Introduction

Investigations of the early events in human immunodeficiency virus (HIV) infection can provide important clues to understanding the resultant disease progression and prognosis (Fauci, 1993; Graziosi et al., 1998; Pantaleo et al., 1993). However, detailed studies of HIV-infected humans at the early stage are extremely limited and even impossible to conduct during the first few weeks (Madea et al., 1990; Prevot et al., 1992). Simian immunodeficiency viruses (SIVs) are closely related to HIVs and some of them are known to cause a fatal disease in infected macaques similar to those seen in human acquired immunodeficiency syndrome (AIDS) (Daniel et al., 1985; Letvin et al., 1985; Letvin and King, 1990; Ringler et al., 1989; Wyand et al., 1989). Extensive studies on the early infection course have been done in macaques to help understand the early infection course in humans (Chakrabarti et al., 1994; Lackner et al., 1994). However, the immune response of monkeys to SIV envelope proteins is thought to be different from the immune response of humans to HIV-1 (Weiss et al., 1986). Thus, for developing anti-HIV-1 drugs and vaccines and for evaluating their efficacy and safety, a new animal model that utilizes the HIV-1 genes would be valuable.

To establish an experimental vaccination model using HIV-1 and macaque monkeys, we have developed a series of SIVmac/HIV-1 chimeric viruses (SHIVs) (Haga et al., 1998; Igarashi et al., 1996, 1994; Sakuragi et al., 1992; Shibata et al., 1991). One of these viruses, NM-3rN, carries

* Corresponding author. Fax: +81-75-761-9335.
E-mail address: tmiura@virus.kyoto-u.ac.jp (T. Miura).
[1] Present address: Department of Pathology, Division of Pathophysiology, Institute of Development, Aging and Cancer, Tohoku University.

0042-6822/03/$ – see front matter
doi:10.1016/S0042-6822(02)00082-X

the region of intact HIV-1 (NL432) that contains *vpr, tat, rev, vpu,* and *env* (Kuwata et al., 1995). In human and macaque peripheral blood mononuclear cells (PBMCs) as well as in some human T-cell lines, NM-3rN replicated effectively. Its replication was comparable to that of SIVmac239 in vitro. NM-3rN-infected monkeys exhibited viremia and the virus was consistently reisolated from these monkeys during the first several weeks postinfection. Nevertheless, none of the infected monkeys showed significant CD4+ T cell depletion or developed AIDS during more than three years of observation (Haga et al., 1998; Hayami et al., 1999). Taken together, these results indicated that NM-3rN should be classified as a persistently infecting but nonpathogenic SHIV.

In addition to being used to develop HIV vaccine candidates, SHIVs have also been used in vivo to explore the pathogenicity of HIV-1 (Harouse et al., 2001; Igarashi et al., 1999; Joag et al., 1996; Reimann et al., 1996a). Reimann et al. succeeded in developing the first pathogenic SHIV (SHIV89.6P) by serial in vivo passages of the original SHIV-89.6 strain (Reimann et al., 1996b). In contrast to NM-3rN, SHIV89.6P replicated much less than SIVmac239 in macaque PBMCs but replicated well in vivo. The virus caused a rapid and profound CD4+ decline within a couple of weeks and then caused miscellaneous opportunistic infections. Thus, SHIV89.6P was considered an acute pathogenic virus. In a postmortem histopathological examination 169 days postinoculation (dpi), Reimann et al. (1996a, b) observed severe thymic dysinvolution and marked histiocytic paracortical expansion in the infected lymph nodes (LNs). However, the mode of disease progression in the early phase of infection was not clear.

The objective of this study was to clarify the early pathological events in both acute pathogenic and nonpathogenic SHIV-infected lymphoid tissues. We inoculated young rhesus macaques with the acute pathogenic SHIV89.6P or the nonpathogenic NM-3rN and compared the results with those obtained from monkeys infected with a chronic pathogenic molecular clone, SIVmac239. We examined the animals by sequential biopsies and by serial necropsies to explore the histopathology and virus distribution in the lymphoid organs. We observed distinct pathological findings and distinct virus-positive cell populations that reflect the marked difference of their virulence.

Results

Peripheral CD4+ cell count and plasma virus load of infected animals

In all four SHIV89.6P-infected monkeys, peripheral blood CD4+ T cells were depleted within 2 weeks (Fig. 1). Two out of three SIVmac239-infected animals showed a transient CD4+ T cell decline while NM-3rN-infected macaques did not show any significant change of CD4+ T cell counts. As the CD4+ cells were declining in the SHIV89.6P-infected monkeys, the viruses were actively replicating. By the end of the second week, the viruses reached their peak levels, more than 10^9 viral RNA copies per milliliter. In contrast, the peak virus load in the NM-3rN-infected monkeys was delayed and less than 10^7 copies/ml, while the peak titer of SIVmac239-infected monkeys showed intermediate properties (the peak titer of the SIVmac239-infected monkeys at 7 dpi was lower than the peak titer of SHIV89.6P-infected monkeys at 14 dpi but higher than that of NM-3rN-infected monkeys at 18 or 23 dpi). Acute infections with the inoculated viruses were also confirmed by virus reisolation at 14 and 21 dpi in all of these animals.

Histopathological changes of the infected thymus

Both of the SHIV89.6P-infected monkeys that developed AIDS (MM130 and MM131) had severe thymic involution (Table 1). Figure 2A shows representative thymic alterations at the AIDS stage caused by SHIV89.6P infection. The thymic parenchyma showed complete obsolescence and was replaced by aggregations of foamy histiocytes. Although the thymuses of the two SIVmac239-infected animals (MM082 and MM105) showed moderate thymic involution (Table 1 and Fig. 2B, left), they showed severe pneumonia and *Pneumocystis carinii* pneumonia around 630 dpi and were judged as having AIDS (Fig. 2B, right). In contrast to these pathogenic viruses, NM-3rN-infected monkeys did not show any symptoms associated with AIDS during an observation period of more than 3 years (Table 1). To understand how the virus-infected organs changed during the early stage of infection, the SHIV89.6P-infected thymuses were examined at 14 and 28 dpi. In both monkeys necropsied at 14 dpi, we observed acute thymic involution with a "starry sky" appearance in the cortex (Table 2, Fig. 3A, left and middle). The so-called starry sky appearance was due to the abundance of tingible-body macrophages in the cortex. This was consistent with our observation of a significant increase of apoptotic cells in the infected cortex at 14 dpi (Iida et al., 2000). Expansion of the medulla was observed with infiltrations of neutrophilic inflammatory cells that were associated with the nuclear debris of dead cells (Fig. 3A, right). Subsequently, the continuous progression of thymic involution resulted in severe atrophy at 28 dpi (Table 2 and Fig. 3C, left). Thus, acute thymic involution began within 14 dpi and resulted in an accelerated thymic atrophy. In contrast to the SHIV89.6P-infected animals, neither the NM-3rN-infected animals nor the SIVmac239-infected animals developed thymic alterations to such an extent within the observation periods (Table 2, Fig. 3C, middle and right). These findings in the SIVmac239-infected thymuses were consistent with the findings of a previous report (Lackner et al., 1994).

The tissue distribution of the virus-producing cells (VPCs) in the infected thymuses was analyzed by histo-

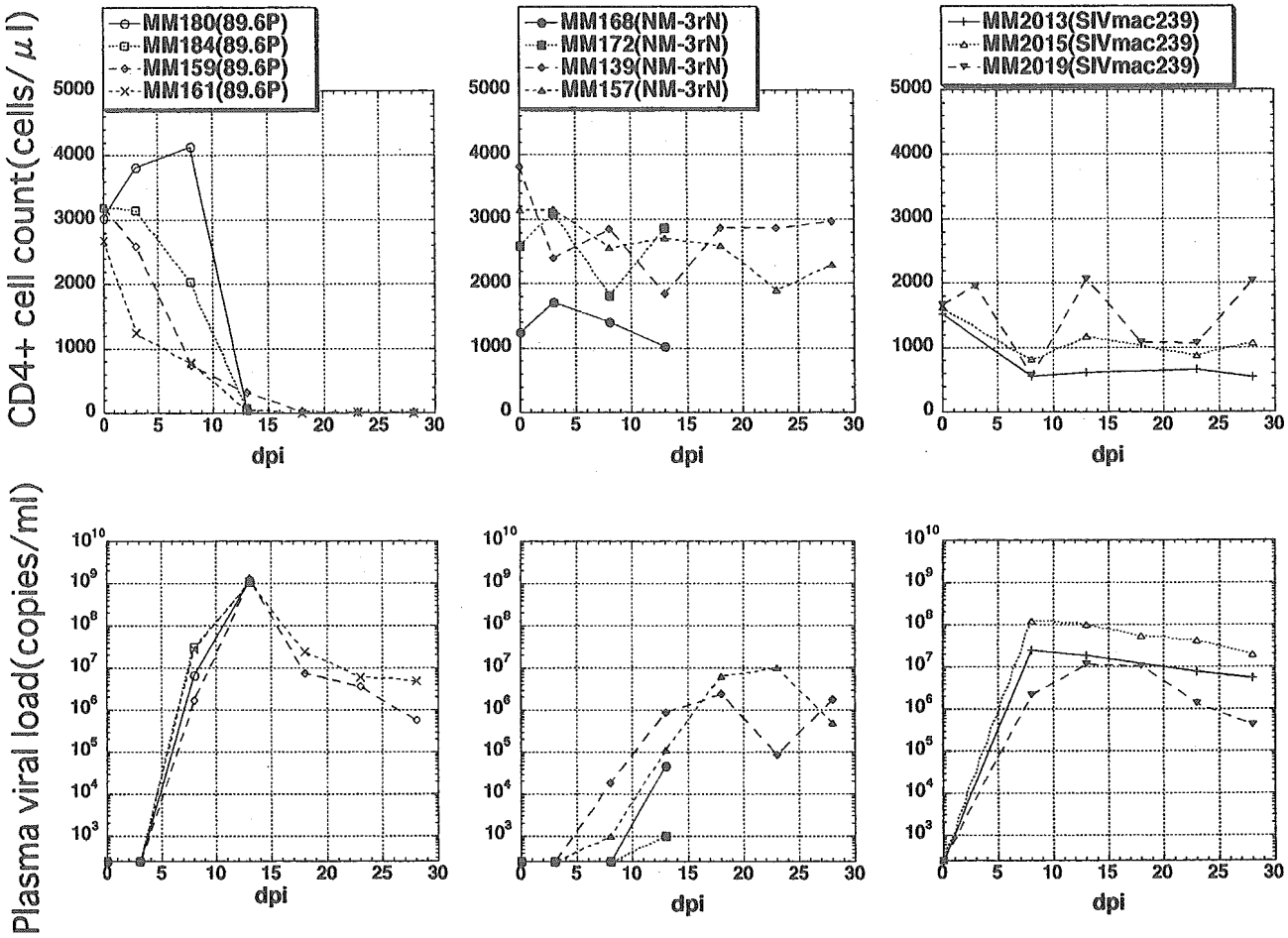

Fig. 1. Kinetics of the peripheral CD4+ cell counts and plasma virus loads in each of the virus-infected monkeys. These parameters were monitored during the observation period of each monkey up to the day of sacrifice.

chemical in situ hybridization (HISH). As shown in Figs. 3B and 3C, in the SHIV89.6P-infected monkeys, the VPCs were localized mainly in the thymic medulla at 14 and 28 dpi. At 14 dpi, the VPCs showed a spindle morphology and were arranged in a network pattern adjacent to Hassall's corpuscles, while much fewer VPCs were observed in the cortex (Fig. 3B). At 28 dpi, the VPCs were scattered in the thymic medulla (Fig. 3C left). The appearance of these VPCs was also associated with the cystic degeneration of the Hassall's corpuscles. In contrast to the pathogenic virus-infected thymuses, the NM-3rN-infected thymuses had only a few VPCs per section (Fig. 3C, middle). In the SIVmac239-infected animals, no obvious histological alteration was observed but scattered VPCs with a small round morphology were identified mainly in the medulla (Fig. 3C, right).

Thymic epithelial cells of the SHIV89.6P-infected monkey, as observed with transparent electron microscopy (TEM), were morphologically classified according to a previous description (Shimosato and Mukai, 1997) (Fig. 4).

Table 1
Disease states of SHIV- and SIV-infected monkeys that were observed for periods of 6 months or more

Animal ID	Inoculated virus	Observation period	Disease state
MM130	SHIV/89.6P, 10 $TCID_{50}$ IV[a]	182 days	AIDS
MM131	SHIV/89.6P, 10 $TCID_{50}$ IV	287 days	AIDS
MM043	SHIV/NM-3rN, 10^5 $TCID_{50}$ IV	1239 days	AC[b]
MM064	SHIV/NM-3rN, 10^5 $TCID_{50}$ IV	1239 days	AC
MM082	SIVmac239, 10^5 $TCID_{50}$ IV	630 days	AIDS
MM105	SIVmac239, 10^5 $TCID_{50}$ IV	630 days	AIDS

[a] IV, intravenous inoculation.
[b] AC, asymptomatic carrier.

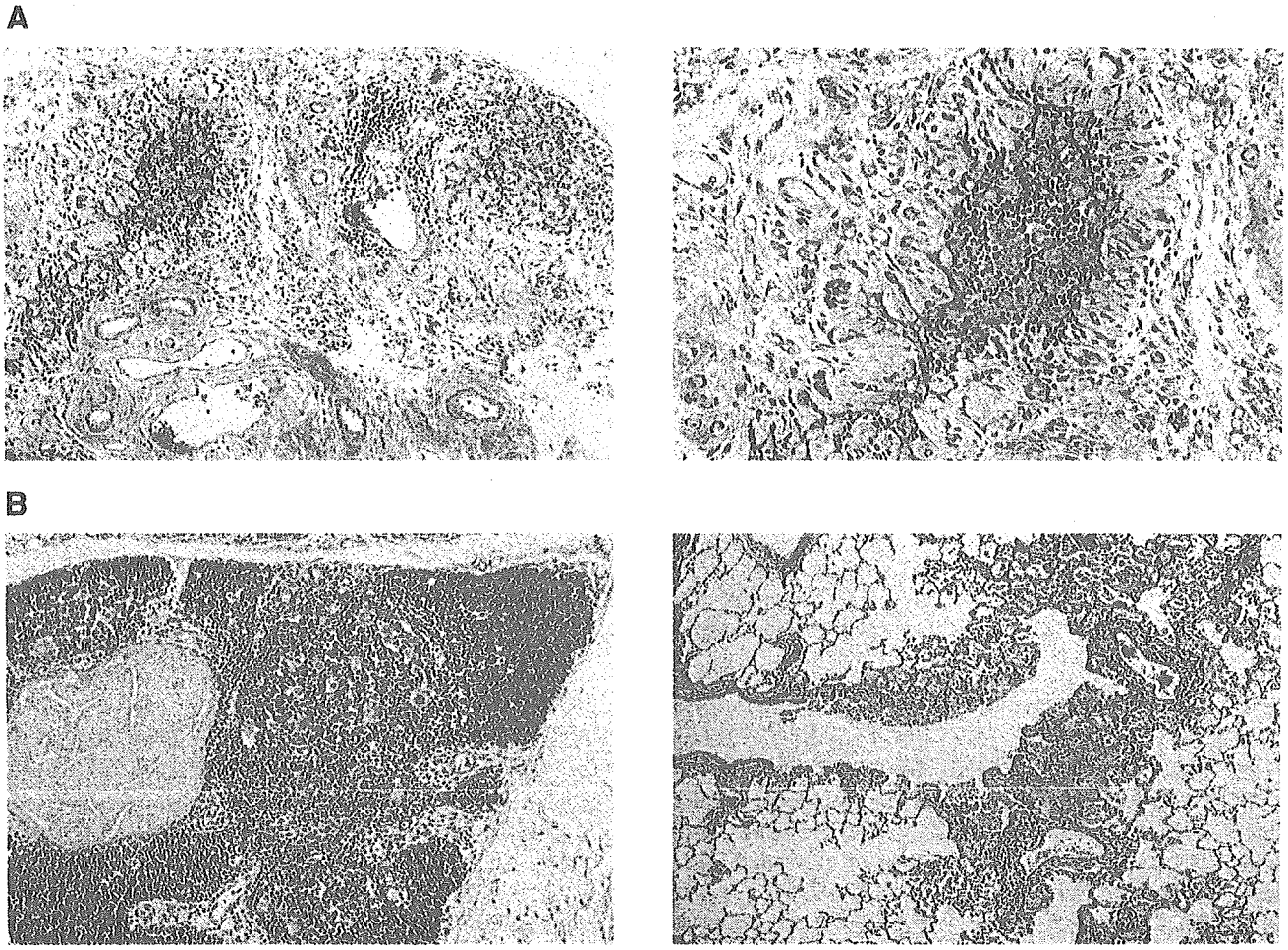

Fig. 2. (A) Involuted thymus in the SHIV89.6P-infected monkey after developing AIDS (MM131). Hematoxylin- and eosin staining (H&E): left, ×40; right, ×400. (B) The involuted but not completely obsolescent thymus derived from a SIVmac239-infected monkey that developed AIDS (MM105; left, ×40). Right panel shows the lung of the same monkey. The terminal airways were filled by *Pneumocystis carinii* (H&E, ×40).

The dark epithelial cells (E4) adjacent to Hassall's corpuscles (H) and the large medullary epithelial cells (E6) seemed to be well preserved at 14 dpi (Fig. 4, left). At 28 dpi, the E4 cells were shrunken and the network structure was distorted (Fig. 4, upper right). In contrast, the subcapsular E1 and pale E2 cell network in the outer cortex seemed to be rather preserved (Fig. 4, lower right). Thus, the disappearance of the VPCs seemed to be in proportion to the disorganization of the thymic medullary epithelial cells.

Histopathological changes of the infected lymph nodes (LNs)

In the SHIV89.6P-infected LNs, remarkable morphologic change was evident from 14 dpi (Table 3 and Fig. 5, upper left). At 14 dpi, the infected nodes revealed a relative paracortical expansion with infiltration of mixed cell types, and there was a severe cell loss at 28 dpi (Fig. 5, lower left). Unlike the HIV- and/or SIV-infected LNs, there was no association of the florid follicular expansion followed by severe involution and depletion. In contrast to the profound CD4+ T cell decline in the peripheral blood within 14 dpi, the cell density in the LNs was rather constant. On the other hand, the NM-3rN-infected LNs showed gradual paracortical expansion at 14 and 28 dpi (Table 3 and Fig. 5, middle). The histology was consistent with chronic nonspecific lymphadenitis and seemed to show mild lymphoid activation. Nevertheless, within this observation period, none of the NM-3rN-infected LNs developed paracortical depletion as the pathogenic SHIV89.6P-infected animals did. The SIVmac239-infected animals exhibited paracortical expansion and sinus histiocytosis at 28 dpi and did not develop the florid follicular hyperplasia that was seen in the persistent generalized lymphadenopathy (PGL) state (Table 3 and Fig. 5, right).

Most of the LNs examined by HISH showed VPCs. The VPCs were mainly in the paracortex, but the ways in which the distributions changed with time differed among the viruses. As previously reported (Chakrabarti et al., 1994; Lackner et al., 1994), in the SIVmac239-infected animals, most of the VPCs were identified in the paracortex at 28 dpi (Table 3 and Fig. 5, lower right). This was more frequent

Table 2
Histopathology and distribution of virus-producing cells in infected lymphoid organs

Virus	Animal ID	dpi	Thymus		Spleen		Tonsil	
			Histopath C/M	HISH C/M	Histopath FL/PALS/RP	HISH FL/PALS/RP	Histopath FL/IF	HISH FL/IF
SHIV89.6P	MM180	14	TBM/IN	+/+++	NP/HM/NP	−/+/−	NA	NA
	MM184	14	TBM/IN	NA	H/HM/NP	−/−/−	H/HM	−/−
	MM159	28	MA/SA	+/++	DP/DP/NP	−/+/−	DP/DP	−/±
	MM161	28	MA/SA	+/++	DP/DP/NP	−/−/−	NA	NA
NM-3rN	MM168	14	NP/NP	−/−	NP/HM/NP	−/−/−	H/HM	−/−
	MM172	14	NP/NP	−/−	H/HM/IN	−/±/−	H/HM	−/±
	MM139	28	NP/NP	−/−	H/NP/NP	±/±/−	H/HM	±/±
	MM157	28	NP/NP	−/−	NP/NP/NP	−/−/−	H/HM	−/−
SIVmac239	MM2013	28	NA	NA	NP/NP/IN	−/±/−	H/HM	+/++
	MM2015	28	NP/NP	−/+	NP/HM/IN	−/+/−	NP/HM	+/++
	MM2019	28	NA	NA	H/HM/IN	−/+/−	H/HM	+/+++

Note. Abbreviations for anatomical sites: C, cortex; M, medulla; FL, follicles; PALS, periarteriolar lymphoid sheath; RP, red pulp; IF, interfollicular area. Histopath, histopathological grading for lymphoid morphology. The histopathological findings for each component are indicated as follows: NP, normal appearance; TBM, tingible body macrophages; IN, infiltration of the neutrophils; MA, moderate atrophy; SA, severe atrophy with lobular collapse; HM, hyperplasia with mixed cell infiltration; H, hyperplasia; DP, depletion; NA, samples not available for study. HISH, histochemical in situ hybridization. Results of HISH were quantified as follows: (−) no positive cell; (±) 1 to 5 positive cells per section; (+) 1 to 5 positive cells per high-power field (HPF = ×400 magnification); (++) 6 to 15 positive cells per HPF; (+++) greater than 15 positive cells per HPF.

than that observed in thymic medulla (Fig. 3C, right). This finding was also consistent with the findings of previous reports (Karr et al., 1994). In the SHIV89.6P-infected LNs, the VPCs transiently increased in number and intensity at 14 dpi and then decreased at 28 dpi. This seemed to be caused by a massive cell loss in the paracortex (Table 3 and Fig. 5, left). On the other hand, in the NM-3rN-infected LN, very few VPCs were detected in the paracortex at 14 and 28 dpi (Fig. 5, middle).

Histopathological changes of the infected spleen and tonsils

It is thought that one of the functions of the spleen is to protect individuals from blood-borne pathogens. The splenocytes are also the target in humans infected with HIV and in monkeys infected with SIV. As reported previously, in the SIVmac239-infected spleen, the VPCs were mainly identified in the periarteriolar lymphoid sheath (PALS), which is a T-cell-dependent zone (Table 2). The SHIV89.6P-infected spleens also exhibited a severe cell loss of PALS at 28 dpi, apparently in parallel with the paracortical depletions in the peripheral LNs. Half of the SHIV89.6P-infected animals showed VPCs in the PALS. In contrast, the NM-3rN-infected spleens exhibited few VPCs distributed in the PALS and showed nonspecific lymphoid activation but never exhibited severe cell loss during the observation periods.

It has been reported that HIV-1-induced changes were more accelerated in the tonsils than in the peripheral LN (Wenig et al., 1996). In three SIVmac239-infected monkeys that were tested in this study, the numbers of VPCs in the tonsils were almost the same as the numbers seen in the corresponding peripheral LNs (Tables 2 and 3). In the SHIV89.6P-infected tonsils, there was clear depletion of mononuclear cells in the paracortex by 28 dpi while only a few VPCs were identified in the same area. On the other hand, in the NM-3rN-infected tonsils, lymphoid activation was the main feature and the frequency of the VPCs was as low as it was in other lymphoid tissues. These findings seem to be similar to what was observed in the paracortex of the peripheral LNs.

Amount of proviral DNA in lymphoid tissues

The amounts of proviral DNA in some lymphoid tissues of infected monkeys were examined by TaqMan PCR (Fig. 6). As expected, the amounts of proviral DNA of all tissues examined were much higher in SHIV89.6P-infected monkeys than in NM-3rN-infected monkeys at all stages. The amounts of proviral DNA in NM-3rN-infected lymphoid tissues were kept at quite low levels during the observation period. In both virus-infected monkeys, the amount of provirus tended to be higher in the thymus than in the spleen and mesenteric LNs at the acute phase of infection, while it tended to be higher in mesenteric LNs at the late stage.

Discussion

The early stage of SHIV89.6P infection was clinically characterized by rapid, profound, and continuous peripheral CD4+ T cell depletion. Reimann et al. (1996a) observed severe thymic dysinvolution (marked atrophy and thymocyte depletion according to their designation) in SHIV89.6P-infected monkeys after 169 dpi. We also noted thymic atrophy and severe paracortical depletion of the peripheral lymph nodes in animals that had developed AIDS. However, the mode of disease

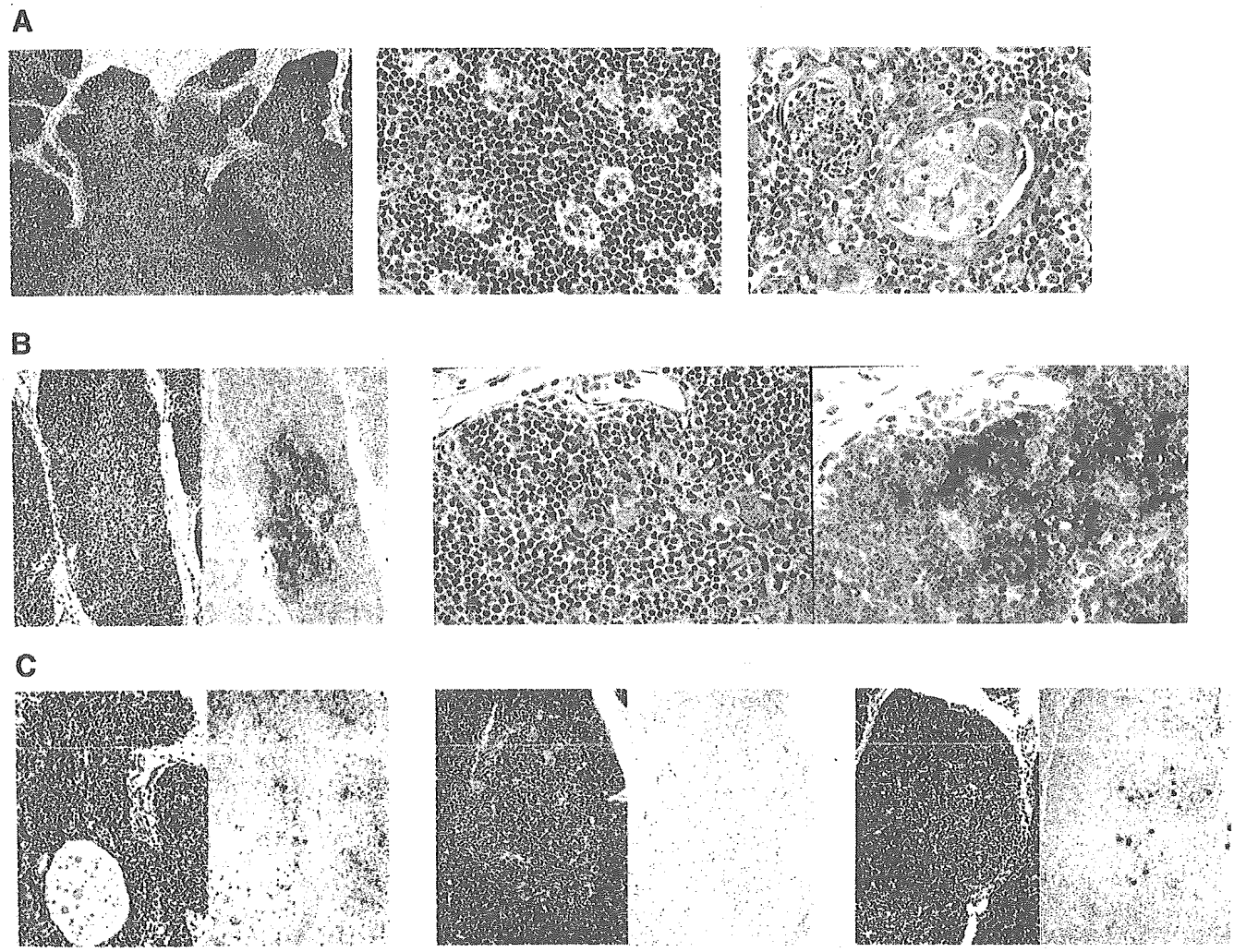

Fig. 3. (A) Representative histology of the early stage of SHIV89.6P-infected thymuses at 14 dpi (H&E). (Left) ×40; (middle) cortex region, ×400; (right) medulla region, ×400. (B, C) Intrathymic distribution of VPCs in the early stage of infection. H&E on left side and histochemical in situ hybridization (HISH) staining on right side are shown, respectively. (B) SHIV89.6P-infected thymus at 14 dpi (left, ×100; right, ×400). (C) SHIV89.6P-infected (left), NM-3rN-infected (middle), and SIVmac239-infected (right) thymus at 28 dpi (×100).

progression was not clear, especially in the early phase of infection. Notably, even the SIV-infected animals that had developed AIDS did not show as much thymic atrophy as was observed in the SHIV89.6P infected animals. In this study, we examined the early stage of pathogenic and nonpathogenic SHIV infections.

All four SHIV89.6P-infected monkeys exhibited severe CD4+ T-cell loss in PBMCs within 14 dpi. Interestingly, despite this observation, the histology of LNs showed paracortical expansion with infiltration of mixed cell types, and the paracortical depletion was delayed to 28 dpi. The peak incidence of the VPCs identified by the HISH analyses seemed to be lower than that seen in the SIVmac239-infected LNs. In fact, most of them disappeared by 28 dpi. Their disappearance was proportional to the paracortical depletion. The paracortical depletion was not found to be associated with either the florid follicular hyperplasia or the resultant follicular depletion, although this type of lesion was usually seen in the SIVmac239 infections. These findings suggest that the profound CD4+ cell depletion in the peripheral blood is a direct reflection of the cell loss caused by the SHIV89.6P infection rather than by redistribution of the infected cells. Wallace et al. (1999) reported that CD4+ T cells are highly activated during acute infection with SHIV89.6PD (a separate isolate of SHIV89.6P) and are unusually susceptible to activation-induced cell death. We previously observed an increased frequency of apoptotic cells in the SHIV89.6P-infected LNs and thymic cortex at the early stage of the infection (Iida et al., 2000). Together, the severe paracortical cell loss without follicular activation seemed to be caused by apoptotic cell death. The high frequency of apoptotic cell death could not be explained only by the cell death directly due to infection with SHIV89.6P because of the low incidence of VPCs.

Our observations indicated that acute thymic involution with a "starry sky" appearance in the cortex prior to severe atrophy was one of the most characteristic in the early stage of SHIV89.6P infection. Thymic involvement has been re-

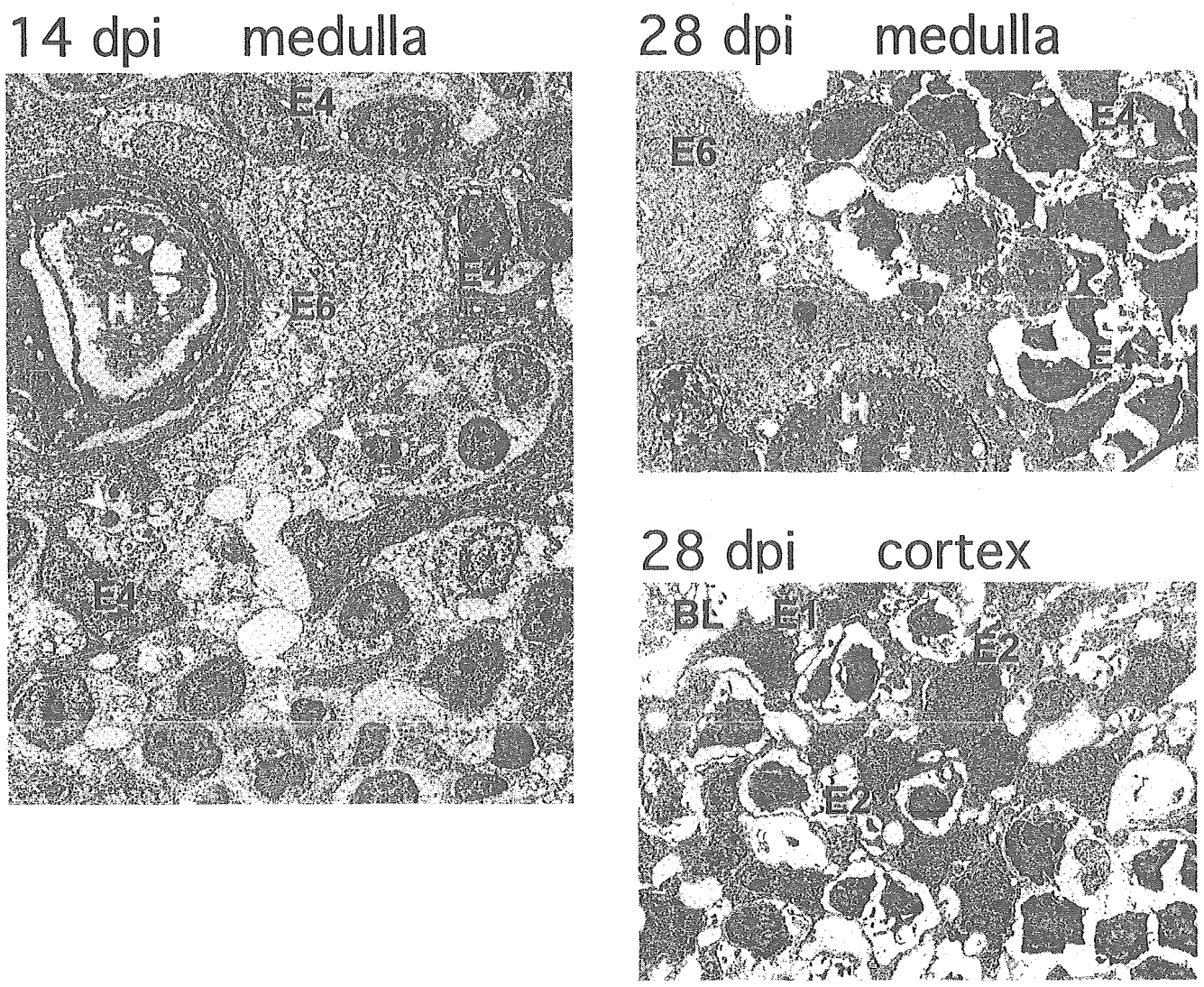

Fig. 4. Representative TEM images derived from SHIV89.6P-infected thymuses at 14 dpi (left) and 28 dpi (right) (×1600). E1, subcapsular cells; E2, pale cells; E4, dark epithelial cells; E6, large medullary epithelial cells; H, Hassall's corpuscles; and BL, basal lamina. The morphological classification of the thymic epithelial cells was according to the reference Shimosato and Mukai (1997).

ported in humans (Burke et al., 1995; Prevot et al., 1992), in macaques (Li et al., 1995; Muller et al., 1993; Wykrzykowska et al., 1998), and in HIV-1-infected thymic implants in SCID-hu mice (Bonyhadi et al., 1993; Ogura et al., 1996). The three major features of the thymic alterations in HIV-infected children and infants are thymitis, precocious thymic involution, and thymic dysinvolution (Joshi et al., 1986). The thymitis was attributed to the formation of lymphoid follicles in the infected medullae. This was observed at a relatively late stage of SIVsm-infected cynomolgous monkeys and seropositive asymptomatic drug addicts (53 to 783 dpi, respectively) (Li et al., 1995; Prevot et al., 1992). One of these studies (Wykrzykowska et al., 1998) described scattered VPCs exhibiting a lymphoid morphology in the medulla as early as 7 dpi. The SHIV89.6P-infected thymuses at this stage did not show a significant follicular aggregation in the medullae as was observed in the SIV-infected animals. Instead, the thymus revealed an abundance of tingible-body macrophages in the cortex accompanied by various degrees of neutrophilic infiltration in the medulla at 14 dpi. This alteration was followed by thymic involution with reduction of VPCs at 28 dpi. Interestingly, the VPCs that were identified in the infected medulla had a spindle shape and a network distribution. Morphologically these seemed to be thymic stromal cells. Similar cell populations and a similar tissue distribution were described in HIV-1-infected thymic implants in SCID-hu mice (Bonyhadi et al., 1993; Okamoto et al., 1998). We noted the peripheral lymphoid depletion in the LNs, spleens, and tonsils in the early stage of SHIV89.6P infections. Taken together, these results seem to indicate that the acute phase of SHIV89.6P infection is characterized by acute thymic involution with generalized lymphoid depletion. In humans, an acute "stress" involution was noted in children undergo-

Table 3
Histopathology and distribution of virus producing cells in sequentially resected peripheral lymph nodes

Virus	Animal ID	Pre-inoculation		5 dpi		14 dpi		28 dpi	
		Histopath FL/PC/S	HISH FL/PC/S	Histopath FL/PC/S	HISH FL/PC/S	Histopath FL/PC/S	HISH FL/PC/S	Histopath FL/PC/S	HISH FL/PC/S
SHIV89.6P	MM180	NP/NP/NP	−/−/−	NP/NP/NP	−/−/−	NP/HM/SH	−/+/−	NA	NA
	MM184	NP/NP/NP	−/−/−	NP/NP/NP	−/−/−	NP/HM/SH	−/+/−	NA	NA
	MM159	NP/NP/NP	−/−/−	NP/NP/NP	−/−/−	NP/HM/SH	−/+/−	H/DP/SH	−/−/−
	MM161	NP/NP/NP	−/−/−	NP/NP/NP	−/−/−	NP/HM/SH	−/+/−	H/DP/SH	−/−/−
NM-3rN	MM168	NP/NP/NP	−/−/−	NP/NP/NP	−/−/−	NP/NP/NP	−/−/−	NA	NA
	MM172	NP/NP/NP	−/−/−	NP/NP/NP	−/±/−	NP/NP/NP	−/−/−	NA	NA
	MM139	NP/NP/NP	−/−/−	NP/NP/NP	−/−/−	NP/NP/NP	−/−/−	NP/H/SH	−/+/−
	MM157	NP/NP/NP	−/−/−	NP/NP/NP	−/−/−	NP/NP/NP	−/−/−	NP/H/SH	−/−/−
SIVmac239	MM2013	NP/NP/NP	−/−/−	NP/NP/NP	−/−/−	NP/H/SH	−/+/−	NP/HM/SH	+/+++/−
	MM2015	NP/NP/NP	−/−/−	NP/NP/NP	−/−/−	NA	NA	NP/HM/SH	+/++/−
	MM2019	NP/NP/NP	−/−/−	NP/NP/NP	−/±/−	NP/H/SH	−/+/−	NP/HM/SH	−/±/−

Note. Abbreviations for anatomical sites: FL, follicles; PC, paracortex; S, sinus. Histopath, histopathological grading for lymphoid morphology. The histopathological findings for each component are indicated as follows: NP, normal appearance; HM, hyperplasia with mixed cell infiltration; SH, sinus histiocytosis; H, hyperplasia; DP, depletion; NA, samples not available for study. The frequencies of VPCs in tissue sections detected by HISH are indicated as described in Table 2.

ing major stress, such as occurs with extensive thermal injury, radiotherapy, anti-tumor therapy, chorioamnionitis, and sepsis (Shimosato and Mukai, 1997; Suster and Rosai, 1992; Toti et al., 2000). The histology of the stress involution was known as acute cortical shrinkage associated with a starry sky appearance, and it was similar to that seen in the SHIV89.6P infection (Fig. 3A and Toti et al., 2000). This accidental or stress-associated involution appears to result from a sudden release of corticosteroid from the adrenal cortex, which causes rapid lympholysis of the cortical thymocytes (Cowan and Sorenson, 1964). Some of the thymic epithelial cells were thought to be secreting thymic peptides, such as thymosin fraction 5, which modulate the hypothalamo–pituitary–adrenal axis by affecting the release of adrenocorticotropic hormone (Goya et al., 1993). Interestingly, we observed densely packed VPCs in the thymic medulla followed by the disruption of the E4 cell network in the SHIV89.6P-infected animals. As mentioned above, the virus did not seem to directly kill many infected cells in the lymph nodes. Taken together, these results suggest that the CD4 depletion in the SHIV89.6P-infected animals is due to stress involution induced by viral infection and that the generation of CD4+ cells in its lineage is inhibited. Expression of interleukin-7, a cytokine produced by thymic stro-

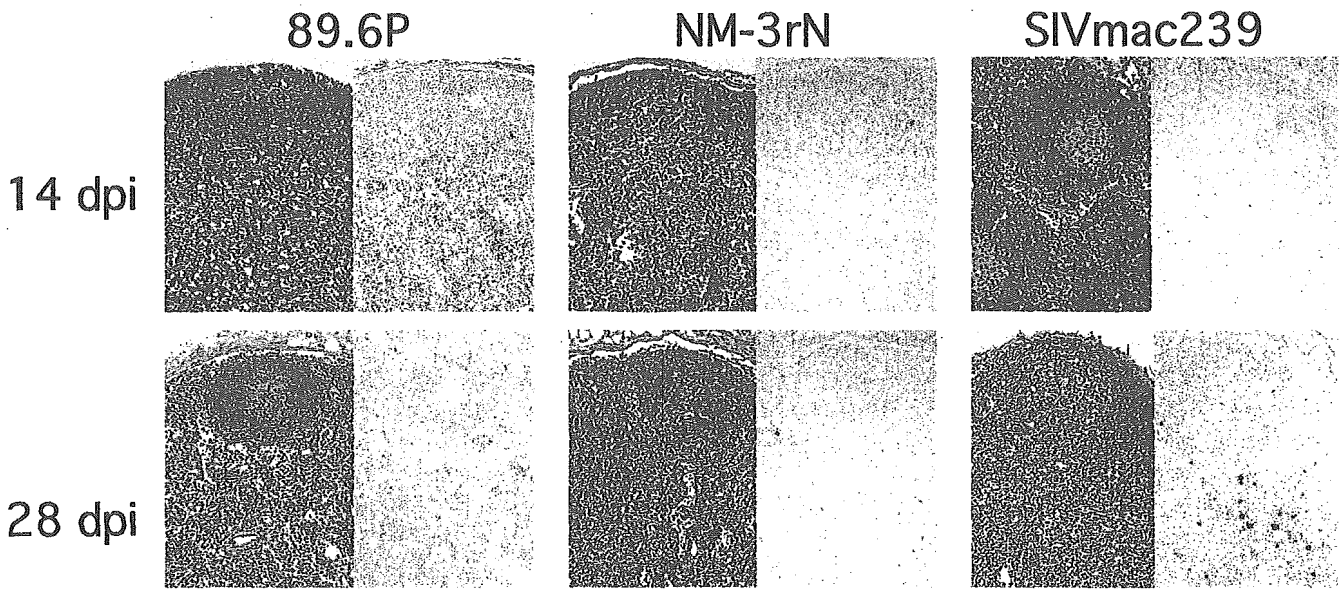

Fig. 5. Representative tissue distributions of VPCs in sequentially resected LNs. The HISH staining of the sequentially resected LNs is shown. SHIV89.6P-, NM-3rN-, and SIVmac239-infected LNs are arranged from left to right, respectively. The left-side image in each panel shows H&E at the indicated period, while the right-side image shows HISH of sequential sections.